



This work is protected by copyright and other intellectual property rights and duplication or sale of all or part is not permitted, except that material may be duplicated by you for research, private study, criticism/review or educational purposes. Electronic or print copies are for your own personal, non-commercial use and shall not be passed to any other individual. No quotation may be published without proper acknowledgement. For any other use, or to quote extensively from the work, permission must be obtained from the copyright holder/s.

THEORETICAL STUDIES OF VACANCY PAIR CENTRES

IN THE ALKALINE EARTH OXIDES

by

Kin Ching To

A thesis

submitted to the University of Keele  
for the Degree of Doctor of Philosophy

Department of Physics,  
University of Keele,  
Staffordshire.

October, 1969.

UNIVERSITY  
OF KEELE



## **IMAGING SERVICES NORTH**

Boston Spa, Wetherby  
West Yorkshire, LS23 7BQ  
[www.bl.uk](http://www.bl.uk)

The following pages have been redacted from the is digital copy, at the request of the university:

Article from: The Physical Review, 1969, vo1.181, no.3 (at end of thesis).

## ACKNOWLEDGEMENTS

The author wishes to express his gratitude to Dr. B. Henderson for his excellent supervision and his patience in reading through this thesis, also Dr. A.M. Stoneham with whose help the author spent a most interesting and instructive summer at Harwell where this work first started. His guidance has been most helpful since.

The author also wishes to express his gratitude to the University Authorities for their offer of a studentship which enabled this work to be done without financial difficulties, and for many other facilities provided by the University.

Thanks also go to Professor D.J.E. Ingram and Dr. D.C. Laine for their excellent lectures that first introduced the author into this field.

Thanks are also due to Miss S.A. Leese for her typing of this thesis.

## CONTENTS

	ABSTRACT	1
<u>CHAPTER I</u>	<u>INTRODUCTION</u>	2
1.1	Defects in Crystalline Solids	3
1.2	Colour Centre in Crystalline Solids	5
	References	10
<u>CHAPTER II</u>	<u>THEORETICAL STUDIES OF F-CENTRES</u>	
2.1	Preliminary Comments	12
2.2	F-centre in the Alkali Halides	18
2.2.1	Kojima's Calculations for Lithium Fluoride	18
2.2.2	The Work of Gourary and Adrian: The Point- Ion Lattice Approximation	23
2.2.3	Ion Size Corrections	27
2.3	F <sup>+</sup> -centres in Alkaline Earth Oxides	32
2.3.1	Kemp and Neeley's Calculations on Oxides	33
2.3.2	Extension of the Point Ion Lattice Calculation	36
2.3.3	Polarisation and Lattice Distortion Corrections	41
2.3.4	Ion Size Correction for the Alkaline Earth Oxides	49
	References	55

<u>CHAPTER III</u>	<u>EXPERIMENTAL EVIDENCES FOR THE <math>F_C^+</math>-CENTRE</u>	
3.1	E.S.R. Studies of Annealed Crystals	57
3.2	The g-shift and Hyperfine Splitting of $F_C^+$ -centres	59
3.3	Optical Properties of $F_C^+$ -centres	63
	References	64
<u>CHAPTER IV</u>	<u>CONTINUUM MODEL FOR <math>F_C^+</math>-CENTRE</u>	
4.1	Preliminary Comments	65
4.2	Pincherle's Calculations on D-centre	70
4.3.1	Binding Energy of $F_C^+$ -centre in Alkaline Earth Oxides	72
4.3.2	Hyperfine Constants of $F_C^+$ -centre in Alkaline Earth Oxides	74
	References	80
<u>CHAPTER V</u>	<u>POINT ION LATTICE CALCULATION ON <math>F_C^+</math>-CENTRE</u>	
5.1	Point Ion Lattice Model for the $F_C^+$ -centre	81
5.2	Polarisation and Lattice Distortion Correction	85
5.2.1	Depolarisation Factors	87
5.2.2	Electrostatic Field and Energy Changes of the Electron	93
5.2.3	The Lattice Energies	97

5.3	Ion Size Correction	99
5.4	The Hyperfine Constants	101
5.5	Conclusions	103
	References	106
	Appendix	107
	Tables	

ABSTRACT

This thesis is concerned with colour centres, particularly the  $F_C^+$ -centre, in the alkaline earth oxides. The  $F_C^+$ -centre consists of an electron trapped at an anion-cation vacancy pair and is intimately connected with the  $F^+$ -centre, an electron trapped at a single anion vacancy. We emphasise in this thesis the connection between the  $F_C^+$  and  $F^+$ -centres. A theoretical model is developed which represents the  $F_C^+$ -centre as an  $F^+$ -centre perturbed by the presence of a neighbouring cation vacancy. The calculated binding energy of the  $F_C^+$ -centre in the point ion lattice approximation is found to be too large compared with experiment. Corrections due to lattice distortion and polarisation effects taken together lower the binding energy; although the polarisations of the surrounding ions actually increases the binding energy the lattice distortion decreases the binding energy by a slightly larger amount. Reasonable agreement between the experimental and theoretical binding energies is obtained for MgO only after ion size corrections to the point ion model. The axial symmetry of the  $F_C^+$ -centre is best revealed by the ratio of the isotropic hyperfine constants,  $A_{00-1}/A_{010}$ . An attempt has been made to calculate the isotropic hyperfine constant within this model. The results show that whilst the ratio agrees reasonably well with the experiment, the absolute value of the isotropic hyperfine constants

are too large compared with experiment. A slight improvement of the isotropic hyperfine constants is obtained when the ion size effect is taken into account.

A continuum calculation for the  $F_C^+$ -centre, in which the electron is assumed to be trapped in the field of a finite electric dipole immersed in a dielectric medium is also attempted, and the results compare with the point ion model for the  $F_C^+$ -centre.

## CHAPTER I

### 1. Introduction

The alkaline earth oxides are wide band gap insulators ( $E_G \geq 6$  ev) which crystallize into a regular array of positively charged metal ions and negatively charged oxide ions having the face-centred cubic (rocksalt) structure. Although they are highly ionic materials it is likely that they are not so ionic as the monovalent and isostructural alkali halides. A typical alkaline earth oxide is characterised by a filled valence band formed from p-like states on the anion and an empty conduction band arising from s-like states on the cation. The detailed nature of the band structure is a topic deserving active research interest, however it is largely unknown and requires both experimental and theoretical study. One of the most appealing features of these materials is their wide range of optical transparency, which at least for magnesium oxide extends from about 8.0 ev where exciton transitions begin (according to work on powders) into the infra-red where lattice restrahl absorption occurs. Defects including transition ion impurities introduced into the lattice often give rise to absorption bands in this region and can be conveniently studied without the interference of competing absorption by the host.

### 1.1 Defects in Crystalline Solids

Intrinsic lattice defects exist in thermodynamic equilibrium in crystalline materials since their presence lowers the free energy of the crystal mainly consequent upon the increased configurational entropy associated with the number of ways of selecting which lattice sites are defective. Simple thermodynamic arguments<sup>(1)</sup> show that the defect concentration depends exponentially upon temperature according as

$$\frac{n}{N} = A \text{ Exp } \left( - \frac{E}{kT} \right) \quad (1)$$

where  $n$  is the number of defects in a crystal with  $N$  lattice sites,  $E$  is the energy required to produce one defect, and the constant  $A$  is related to the changes in vibrational energy of atoms near to the defect  $E$ , the formation energy determines which defect type, Schottky (single vacancy) or Frenkel (interstitial-vacancy pair) is present in a particular solid. For example, most metals, the alkali halides and alkaline earth oxides experience Schottky disorder since  $E_S > E_F^+$  whereas the opposite situation obtains in the silver halides and some non-stoichiometric oxides.

---

<sup>+</sup>The subscripts  $S$  and  $F$  refer to Schottky and Frenkel defects respectively.

The most obvious manifestation of the presence of defects in solids are the easily measurable changes in crystal density and X-ray lattice parameter. In fact comparison of these changes not only indicates the nature of the lattice disorder but also allows an estimate to be made of the defect formation energy<sup>(2)</sup>.

In pure ionic solids the formation of lattice defects must take place such that charge neutrality be maintained over the volume of the crystal. Thus in an alkali halide crystal, the formation of a Schottky defect must involve a pair of separated vacancies, one anion and one cation, being produced simultaneously, and  $E_S$  then represents the energy required to create such a pair. The Frenkel defect, however, remains unchanged since the interstitial ion is oppositely charged to the vacant site which it formerly occupied. There are, of course, both anion and cation Frenkel defects. The charge associated with these intrinsic defects has other important consequences for the properties of crystals. As a result of the strong electrostatic interaction between an anion and a cation vacancy, it is energetically favourable for them to aggregate together to form a bound pair. Such a pair makes no contribution to ionic conductivity, although it may be important to diffusion processes<sup>(3)</sup>. Other types of defect aggregate may also occur. For example when  $\text{CaCl}_2$  is added to  $\text{NaCl}$  and  $\text{Ca}^{2+}$  ions substitute directly for the unipositive sodium ions, additional cation vacancies being incorporated to offset the excess charge on the divalent impurity ions.

A  $\text{Ca}^{2+}$  ion may then associate with a cation vacancy to form an impurity-vacancy pair: whether the vacancy occupies a nearest neighbour site along a (110) axis or a next nearest neighbour site along a (100) cannot be decided simply by inspection. In potassium chloride the most stable site for the cation vacancy is the next nearest neighbour site, whereas in sodium chloride the nearest neighbour site is favoured. Trivalent ions in magnesium oxide may have the charge compensating vacancy in either site, the next nearest neighbour site being slightly favoured.

## 1.2 Colour Centre in Crystalline Solids

Colour centres in the alkali halides afford a further means of charge compensation for intrinsic lattice defects. The term "colour centre" was used originally by Pohl<sup>(4)</sup> to designate the defects responsible for the characteristic colour of alkali halide crystals after heating in alkali metal vapour. Many investigations subsequent to Pohl's pioneering work have established that the most important defect in these additively coloured crystals consisted of an electron trapped at a negative ion vacancy, the F-centre. The F-centre is analogous to the hydrogen atom, except that the positive charge which traps the electron is distributed over the "cage" of nearest neighbour cations. Thus we can discuss the eigenstates of the F-centre electron in terms of energy levels of the hydrogen atom, and designate

them as the  $|1s\rangle$ ,  $|2s\rangle$ ,  $|2p\rangle$  etc levels obtained by solution of a one electron Schrödinger equation. As we shall see later this is only an approximate description, which must in general be modified to take account of numerous other interactions. However these energy levels, which we describe approximately as  $|1s\rangle$ ,  $|2s\rangle$ ,  $|2p\rangle$  etc occur within the band gap of alkali halide crystals, and electric dipole transitions which occur between them lead to the characteristic colour of crystals containing F-centres. Vacancy pairs may also act as traps for free electrons, thereby reducing the electron mobility. Thus it is interesting to investigate the binding energy of an electron trapped at such a vacancy pair. In general, however, this situation has not been observed in the alkali halides, and our present studies have been concerned with the alkaline earth oxides in which such F-like centres have long been known to exist.

Colour centres are also produced in alkali halide crystals by ionizing radiation. The primary products of such irradiations are F-like centres and  $V_K$ -centres. During irradiation, energy is transferred to anions some of which are ejected into interstitial sites several lattice spacings removed from the vacancies which they had formerly occupied. Free electrons simultaneously produced are then trapped at the anion vacancy so creating F-centres.

The interstitial halide atom usually bonds covalently with an anion to form an  $X_2^-$  molecule ion centred at a single anion site.

Subsequent irradiation with light in the F-band converts F-centres to aggregate centres. There is now considerable evidence that these centres, referred to as M-, R- and N- centres, are aggregates of 2, 3 and 4 F-centres<sup>(5)</sup>. Charged aggregate centres also exist which have either trapped an extra electron or lost an electron by ionization. Thus the three centres  $M^+$ , M and  $M^-$  are structurally identical since each involves two vacancies on neighbouring anion sites; they differ in that they contain respectively one, two, and three electrons.

In the alkaline earth oxides vacant lattice sites bear an effective charge twice that of the corresponding vacancy in the alkali halides. Thus anion vacancies may trap two electrons to form a neutral defect. Such a defect is expected to have bound excited states in contradistinction to the analogue defect, the  $F^-$ -centre in the alkali halides<sup>(6)</sup>. The additional trapping potential of vacancies in the oxides and the different charge state of a particular defect relative to the alkali halides, is an apparent complication in any system of nomenclature based upon that used by research workers in the alkali halides. For example, an oxygen ion vacancy at which a single electron is trapped has similar optical and magnetic properties to the alkali halide F-centres,

despite being effectively positively charged. This centre might be appropriately designated the  $F^+$  -centre. Extending such a system to all defects in the oxides is quite simple using the system of letters developed for the alkali halides, with an appropriate superscript indicating the charge state of the defect. Thus the defects produced by trapping one, two and three electrons in the anion vacancy would be referred to as the  $F^+$ ,  $F$  and  $F^-$  centres respectively. Aggregate centres similar to the M, R and N-centres are also believed to exist in the oxides; the nomenclature developed above is easily adapted to such defects<sup>(7)</sup>.

Although the above system of nomenclature is both a logical and self-consistent extension of that used in the alkali halides, it is not so easily applied to centres which have no direct analogue in the alkali halides. One such centre is the subject of the present investigation. This defect was first reported by Wertz and his associates<sup>(8)</sup> in neutron irradiated samples subjected to annealing treatments above  $570^{\circ}\text{K}$ . In such samples the amplitude of the  $F^+$ -centre E.S.R. spectrum is reduced and a new spectrum shifted from the  $F^+$ -centre spectrum by  $\Delta g = 0.0015$  in magnesium oxide is observed. Wertz et al, suggested that this spectrum and its mode of formation was consistent with cation vacancies migrating to the  $F^+$ -centres to form a vacancy aggregate. In addition to being observed in the four oxides the defect was also detected in MgS, SrS, SrSe and BaSe<sup>(8)</sup>. As we shall see this defect behaves like an

$F^+$ -centre, at least in respect of its E.S.R. spectrum and it is plausible to refer to this as the  $F_C^+$ -centre, the subscript C indicating that one of the cation sites neighbouring the  $F^+$ -centre is vacant. The centre does have symmetry properties similar to the  $F_A$ -centre (F-centre + impurity ion) in the alkali halides since the presence of the vacancy lower the symmetry from octahedral to tetragonal. The similarity is not further manifest in the properties of the  $F_A$ -centre and the  $F_C^+$ -centre.

In this thesis the  $F_C^+$ -centre is treated theoretically as an  $F^+$ -centre perturbed by the presence of the nearby cation vacancy, using a point-ion polarised lattice model. This is physically realistic since the charge cloud is chiefly concentrated in the anion vacancy. The earliest theoretical work on this type of centre was by Pincherle and specifically concerned the D-Centre in silver halides<sup>(9)</sup>. Pincherle treated this defect as an electron trapped in the field of a finite dipole contained in a dielectric continuum. He proceeded using a simple trial wave function and minimized the energy by the variational method. More recent calculations<sup>(10)</sup> follow similar lines except that a more exact solution to the equations governing the electron and the dipole is found. The binding energy of electron to the vacancy pair is then interpolated from the free ion eigenvalues bearing in mind that the centre is immersed in the solid dielectric. This is taken account of in the usual way by scaling all electrostatic forces by the inverse of the dielectric constant.

References

1. N.F. Mott and R.W. Gurney, "Electronic Processes in Ionic Crystals", (Oxford 1940).
2. See for example articles by J.H. Crawford, *Advances in Physics* 17, 93 (1968), L. Esterman, W.J. Lewdin and D. Stern *Phys. Rev.* 75, 627, (1949). R. Balzer, H. Peisl and W. Waidelich, Abstract 12, International Symposium on Colour Centres in Alkali Halides, Rome (1968).
3. L.W. Barr and A.B. Lidiard, *Phys. Chem.* 10, An Advanced Treatise (Academic Press). A.B. Lidiard, *Handbuck der Physik*, 20, 246, 1957.
4. R.W. Pohl, *Proc. Phys. Soc.* 49, 3, (1937).
5. e.g. J.H. Schulman and W.D. Compton, "Colour Centres in Solids" (Pergamon Press, Oxford 1962).  
A.E. Hughes, Ph.D. Thesis, Oxford University (1966).  
W.B. Fowler (Ed), "The Physics of Colour Centres" (Academic Press, New York, 1968).
6. B. Henderson, S.E. Stokowski and T.C. Ensign, *Phys. Rev.*  
(To be published) (1969).
7. B. Henderson and J.E. Wertz, *Advances in Physics*, 17, 744, (1968).

8. J.E. Wertz, J.W. Orton and P. Auzins, *Disc. Far. Soc.*  
30, 40, (1961). *J. App. Phys. (Supp)* 33, 322, (1962).  
P. Auzins, J.W. Orton and J.E. Wertz, "Paramagnetic Resonance"  
edited by W. Low 1, 90, (Academic Press, 1963).
9. L. Pincherle, *Proc. Phys. Soc.* A64, 648, (1951).
10. R.F. Wallis, R.C. Herman and H.W. Milnes, *J. Mole. Spec.* 4,  
51, (1960).  
K.C. To, A.M. Stoneham and B. Henderson, *Phys. Rev.* 181, 1237  
(1969).

CHAPTER II

THEORETICAL STUDIES OF F-CENTRES

2.1 Preliminary Comments

Theoretical calculations of colour centre properties are many-body problems involving interactions between the trapped electrons and both the ion core electrons and nuclei of all lattice ions. This is a formidable task, and the approximations used in actual calculations must always be the subject of close scrutiny. There are in general two approaches, on the one hand continuum approximations neglect all local interactions between the defect and its environment, while on the other hand molecular orbital treatments neglect long range interactions concentrating on the interactions between the electron and some of its closest neighbours. A common feature of all theoretical models, however, is that they attempt to compute one or more of such experimentally measurable quantities as the location, shape and temperature dependence of the optical band, the lifetime and thermal ionization energy of the excited states of the defect, and the magnitude of any hyperfine interactions. The many body calculation is intractable even for the largest computers and the simplifying assumptions used are usually chosen according to which defect properties are to be calculated. Because of its apparent simplicity most calculations have been concerned with the F-centre and the ensuing brief review reflects this.

The earliest calculations of the F-band transition energy used the semi-continuum approximation which largely neglects the periodic crystal lattice. The vacancy is treated as a positively charged cavity embedded in a continuum dielectric medium, the cavity radius  $R$  being obtained from an explicit calculation of the polarisation field<sup>(1)</sup>. Electric field intensities are calculated using the appropriate dielectric constants. Thus once the form of the potential at the vacancy is found for the electron in the cavity, the energy eigenstates of the electrons are found by solving the appropriate Schrödinger equation. Tibbs<sup>(2)</sup> and later Simpson<sup>(3)</sup> used particularly simple forms of the electrostatic potential inside the vacancy and obtained values for the F-centre transition energy in NaCl of 1.26 eV and 2.20 eV respectively. The experimental value is 2.72 eV. Both calculations assumed that the polarization of the lattice depends only upon the time average of the electron's distribution. A later calculation<sup>(4)</sup>, which assumed that the electrons on the neighbouring ions can follow the motion of the trapped electron adiabatically, results in a tighter binding of the electron in the vacancy especially in the  $|1s\rangle$  ground state because the potential arising from the lattice polarization is decreased. The improved F-band transition energy in NaCl is 2.62 eV.

Temperature dependent properties, such as the optical band shape, are best analysed using models based on the adiabatic Born Oppenheimer approximation<sup>(5)</sup> used originally in the treatment of molecules. The method assumes that the total wave functions of the system may be written as the product function,

$$\Psi_{im} = \phi_i(r, Q) \psi_m(Q) \quad (2.1)$$

where  $i$  and  $m$  represents the electronic and vibrational quantum states respectively,  $r$  and  $Q$  are respectively the electronic and nuclear co-ordinates and  $\psi_m$  are wave functions of the harmonic oscillators assumed to represent the lattice phonons. The classical form of the Franck-Condon principle is also assumed to apply, and the electronic wave functions  $\phi_i(r, Q)$  are very slowly varying functions of  $Q$ . Consequently an optical transition between ground and excited electronic states takes place so quickly that the lattice ions are unable to move to the equilibrium position consistent with the excited state during the transition. Calculations assuming that the electrons are coupled either to a continuum of lattice modes or to a single localized mode have been strikingly successful in predicting the detailed band shapes, temperature dependence of the optical transitions and the energy shifts between absorption and emission bands<sup>(6)</sup>. Apart from the localized mode approximation<sup>(7)</sup> the models noted above ignore the detailed interactions of the trapped electron with neighbouring

ions, although magnetic resonance results clearly demonstrate the importance of such interactions. The remarkable successes of the continuum methods are sufficient to convince us of the importance of long range interactions also.

A number of methods have been forthcoming which attempt to include explicitly the interactions of the trapped electron and ion core electrons. For example a molecular orbital technique allows the trapped electron to spend some fraction of its time overlapping onto the neighbouring ions, during which time it is assumed to behave as a valence electron on the cation. The assumed trial wavefunction is a linear combination of the atomic orbital wavefunctions (L.C.A.O.) of the six neighbouring cations, the coefficients of this combination function being used as adjustable parameters<sup>(8)</sup>. Such detailed effects as exchange, polarisation effects and Van der Waals interactions may all be included<sup>(9)</sup>. Gourary and Adrian<sup>(10)</sup> argued that since the F-centre electron spends very little of its time on neighbouring cations, the average wave function is insensitive to exchange and overlap effects between the electron and the ion core electrons. Thus they adopted a method, the point ion lattice approximation (P.I.L.A.) in which the ions are represented as point charges located on the lattice points. The electron trapping potential used in the Schrödinger equation is then determined from the spherically symmetric contribution of all point charges at the site of the vacancy.

They used trial wave functions which were essentially s-like for the ground state and p-like for the excited states, although L.C.A.O. schemes have also been used within the framework of the P.I.L.A.<sup>(14)</sup>. These last two methods are useful for calculating not only the optical properties of F-centre but also the hyperfine interaction constants, at least provided that the wavefunctions of the trapped electron are properly orthogonalized to the wave functions of the ion core electrons.

Despite all the possible assumptions made above, the many-body problem is still to be formulated and this is of crucial importance in deciding the form of the trial wavefunctions used. The two main assumptions which are of proven value for calculating defect properties, and which effectively reduce the many-electron problem to a one electron problem are the Quasi-Adiabatic Approximation and the Hartree-Fock procedure. In essence these assumptions single out the trapped electron for detailed study, while the effect of all other ion core electrons, except perhaps the ion core electrons on the nearest neighbour ions, are replaced by an average effective potential. A particularly clear exposition of these approximations is contained in the review article by Gourary and Adrian<sup>(10)</sup>, and here we only summarise their essential properties. In the Quasi-adiabatic approximations, the trapped electrons are regarded as being much more weakly bound to the

vacancy than are ion core electrons to the neighbouring ions. It is therefore reasonable to assume that the strongly bound, rapidly revolving ion core electrons can follow the detailed motion of the weakly bound F-centre electrons. Conversely the F-centre electron is unable to follow the detailed motion of the core electrons, and is therefore only effected by the average of their motion. The effect of this is that the interaction energy of the trapped electron with the "electron component" of the polarisation is independent of the position of the electron, and therefore may be omitted from the Hamiltonian.

In direct contrast to the Quasi Adiabatic approximation, the Hartree-Fock procedure states that except for correlations imposed by the exclusion principle, every electron moves in an averaged field of all the other electrons. According to the Quasi Adiabatic approximation, the core electrons are able to follow the average motion of the trapped electron only when the correlation polarisation interaction is small. This latter interaction arises from the polarisation of the core electrons by the trapped electron at its instantaneous position reacting back on the trapped electron. This interaction therefore depends on the instantaneous position of the trapped electron. If this interaction is small, then we may assume that the core electron also follows the average motion of the trapped electron, as is the case for F centres.

This initial preamble serves only as a guide to some of the techniques used over about 25 years of study. Inevitably techniques have become increasingly sophisticated during that time and it is not possible here to review comprehensively all the modifications which have occurred. Consequently the more detailed treatment which follows is concerned only with the more important developments, especially those which have been adapted in their use of studies of  $F^+$ -centres in the Alkaline Earth Oxides.

## 2.2 F-centres in the Alkali-Halides

The earliest models applied to the F-centres in the alkali halides were the continuum and semi-continuum models. These models have not been applied to  $F^+$ -centres in oxides and are of historical interest only. The references at the end of this chapter give the relevant details.

### 2.2.1 Kojima's Calculations for Lithium Fluoride

Inui and Uemura<sup>(8)</sup> first treated the F-centre problem from an atomistic viewpoint with their "small" and "large" molecule approximation. Kojima<sup>(9)</sup> made a more extensive use of this technique applying it to the F-centre in LiF. The basis of Kojima's calculation was the quasi adiabatic approximation with the complete Hamiltonian divided into polarisation dependent and independent terms.

The polarisation dependent effects were treated first by Mott and Littleton's zeroth order approximation<sup>(1)</sup> and later by the second order Mott and Littleton procedure<sup>(1)</sup>. The polarisation independent terms in the Hamiltonian included not only the kinetic energy of the trapped electron but also the electrostatic interaction between the F-electron and both the atomic nuclei and the ion core electrons, allowing for any penetration of the trapped electron into the ion cores. In Kojima's notation this part of the polarization independent term is written as

$$\langle H_1 \rangle = -\frac{\hbar^2}{2m} \int \psi \nabla^2 \psi d\tau - e^2 \sum_v Z_v \int \frac{\psi^2(r)}{|r-R_v|} d\tau + 2e^2 \sum_j \int \frac{\psi^2(r) \chi_{v,j}^2(r')}{|r-r'|} d\tau d\tau' \quad 2.2$$

where  $\psi(r)$  and  $\chi_{v,j}$  are wave functions for the trapped electron and the undistorted  $j$ th shell of the  $v$ th ion respectively, and  $Z$  is the atomic number of the  $v$ th ion. The F-electron also interacts with the polarisation induced by the charge vacancy. This is difficult to compute and is conveniently divided in two parts, one part each due to interactions with the infrared and optical components of the induced polarisation. This latter component is constant in the quasi-adiabatic approximation. Since the interaction energy of a dipole  $P$  with an electric field  $E$  is given by,

$$\vec{H} = - \vec{P} \cdot \vec{E} \quad 2.3$$

the total interaction between the trapped electron and the polarisation field is then given as

$$\begin{aligned}
 \langle H_2 \rangle = & - \sum_{\nu} \frac{M_{\nu} e^2 a^3}{R_{\nu}^2} \frac{\partial}{\partial R_{\nu}} \left[ \frac{\psi^2(r) d\tau}{|r-R_{\nu}|} \right] \\
 & - \sum_{\nu} M_{\nu}^0 e^2 a^3 \left| \nabla_{\nu} \left[ \frac{\psi^2(r)}{|r-R_{\nu}|} d\tau \right] \right|^2 \\
 & - \sum_{\nu} (M_{\nu} - M_{\nu}^0) e^2 a^3 \left| \nabla_{\nu} \left[ \frac{\psi^2(r)}{|r-R_{\nu}|} d\tau \right] \right|^2
 \end{aligned} \tag{2.4}$$

In equation 2.4 the first term represents the electron's interaction with the charged vacancy, whilst the second and third terms represent the electron's interaction with the polarization field:  $M_{\nu}^0$  and  $M_{\nu}$  are respectively the optical and infrared components of the polarisability of the  $\nu$ th ion. Kojima also introduced an exchange interaction in the form,

$$\langle H_3 \rangle = - e^2 \sum_{\nu, j} \int \frac{\psi(r) \chi_{\nu j}(r) \psi(r') \chi_{\nu j}(r')}{|r-r'|} d\tau d\tau' \tag{2.5}$$

The total energy of the system is now a simple sum of the energies given by equation 2.2, 2.4 and 2.5 plus the internal energy of the polarised lattice.

A variational calculation was then made using an assumed wave function. Kojima first used an L.C.A.O. wave function comprising the  $|2s\rangle$  and  $|2p\rangle$  orbitals centred on the six nearest neighbour  $\text{Li}^+$  ions surrounding the vacancy. In the octahedral symmetry that is the F-centre, Kojima's ground state wave function was simply

$$\begin{aligned} \psi(r) = a_1 \sum_{k=1}^6 S(r-R_k) + a_2 \{P_x(r-R_1) - P_x(r-R_2) \\ + P_y(r-R_3) - P_y(r-R_4) + P_z(r-R_5) - P_z(r-R_6)\} \end{aligned} \quad 2.6$$

where  $a_1$ , and  $a_2$  are the variational parameters. The excited state wave function was similarly expressed as,

$$\begin{aligned} \psi_e(r) = b_1 \{S(r-R_5) - S(r-R_6)\} + b_2 \sum_{k=1}^4 P_z(r-R_k) \\ + b_3 \sum_5^6 P_z(r-R_k) \end{aligned} \quad 2.7$$

These wave functions violate Pauli's exclusion principle since they are not orthogonal to the core orbitals. In order to obviate this difficulty, Kojima assumed point charges to represent the ions to whose core orbitals the atomic orbitals comprising the trial wave function were not orthogonal. This modification of the potential was not particularly satisfactory and it was found necessary to

orthogonalise the trial wave function to the core orbitals to obtain better agreement with experiment. The calculation gave the following results:

polarisation neglected	:	E = 4.18 ev
polarisation included	:	E = 3.5 ev
experimental value	:	E = 4.96 ev

The agreement between theory and experiment is noticeably poor. To improve this situation, Kojima used a second trial wave function,

$$\psi(r) = f(r) - \sum_{v,j} \chi_{v,j}(r) \int f(r) \chi_{v,j}(r) d\tau, \quad 2.8$$

the envelope function  $f(r)$  being now orthogonalised to the core orbitals  $\chi_{v,j}(r)$ , by the Schmidt process<sup>(11)</sup> In the ground state the envelope function  $f(r)$  was,

$$\begin{aligned} f(r) &= C \sin kr / (kr) & r < R \\ &= C' e^{-\alpha r} & r > R \end{aligned} \quad 2.9$$

where  $\alpha$  is a variational parameter and  $c$ ,  $c'$  and  $k$  are determined from the condition that the two branches of  $f(r)$  should join smoothly at  $r = R$  and from the normalisation of  $f(r)$ . For the first excited state, the envelope function was written as,

$$\begin{aligned} f(r) &= C_e \left( \frac{\sin k_e r}{k_e^2 r^2} - \frac{\cos k_e r}{k_e r} \right) \cos \theta, & r < R \\ &= C_e' r e^{-\alpha_e r} \cos \theta, & r > R \end{aligned} \quad 2.10$$

where  $\theta$  is the polar angle referred to the (1, 0, 0) axis. The value of  $R$  was fixed at  $R = 0.9a$  after Mott and Littleton<sup>(1)</sup>. Later Kojima took the Mott and Littleton procedure to second order, although the calculation became rather cumbersome. In essence the second order correction to the polarisation energy assumes the dipole moments to be unknown. They are then used together with the lattice distortion as variational parameters, in minimising the energy of the system. The result obtained for the transition energy was 4.96 eV, in exact agreement with experiment. The author pointed out that this agreement is somewhat fortuitous. Even so it is rather remarkable.

Despite giving good results for F-centres in LiF, Kojima's calculation is difficult to extend to other systems and to more complex centres, mainly as a result both of the many two centre integrals involved and the non-availability for many ions of interest of Hartree Fock wave functions in analytic form. The point ion model of Gourary and Adrian is therefore of interest because of its simplicity and because it is easily extended to other more complex systems.

#### 2.2.2. The Work of Gourary and Adrian: The Point-Ion-Lattice Approximation

The point-ion-lattice model developed by Gourary and Adrian<sup>(10)</sup> has now become one of the most valuable starting points for theoretical study of defects in ionic solids. In this model the

complete Hamiltonian is replaced by a simplified Hamiltonian in which each finite ion is replaced at its lattice site by an effective point charge of magnitude equal to the valency of the appropriate ion. (The finite ion size and polarisation effects are added later as corrections to this model). The expectation value of the Hamiltonian is then written as,

$$\langle H \rangle = - \frac{\hbar^2}{2m} \int \psi \nabla^2 \psi d\tau + e^2 \sum_v \int \frac{Z_v \psi^2(r)}{|r-R_v|} d\tau \quad 2.11$$

where  $Z_v$  is now the valency of the  $v$ th ion. It is to be noted that equation 2.11 results directly from equation 2.2 under the restriction that the F-electron does not penetrate the ion cores. The physical basis for this can be seen quite simply as follows: If the trapped electron is completely outside the charge distribution of the core electrons, then the electrostatic field which it experiences is just that due to the nucleus surrounded by the core electrons. This potential is equal to that due to a free ion with a net charge equal to its valency.

Gourary and Adrian used group theoretical methods to show (i) that the point ion potential can be expanded in terms of cubic harmonics<sup>(12)</sup> of even order, and (ii) that for the purpose of calculating the ground and first excited state energies, only the spherically symmetric part of the expansion of the point ion potential

is needed. This greatly simplifies the problem. A further simplification occurs because exchange interactions with the core electrons are neglected, there being no counterpart to exchange interactions in classical electrostatics. Thus the trial wave functions for the F-electron need no longer be orthogonalised to the ion core orbitals.

Gourary and Adrian<sup>(10)</sup> used three different sets of envelope functions for the ground and excited states, in order to calculate the energy integrals. These integrals were then minimized with respect to the parameters of the envelope function. The best wave functions, which are written below, were type III wave function for the ground state and type II wave functions for the first excited state: Type III wave function:

$$\begin{aligned}
 Q(\Gamma_1^e, 0, 0 | \theta, \phi) &= \sqrt{\frac{1}{4\pi}} \\
 R(\Gamma_1^e, 0, 0 | r) &= A j_0(\xi r/a) k_0(\eta) \quad r < a \\
 &= A j_0(\xi) k_0\left(\frac{\eta r}{a}\right) \quad r > a
 \end{aligned}
 \tag{2.12}$$

where  $\eta = -\xi \cot \xi$  and  $k_0(x) = e^{-x}/x$ .

Type II wave functions:

$$Q(\Gamma_4^0, 1, 0 | \theta, \phi) = \frac{\sqrt{3}}{4\pi} \cos \theta$$

$$R(\Gamma_4^0, 1, 0 | r) = A' j_1(\xi' \frac{r}{a}) e^{-\eta' r} \quad r < a \quad 2.13$$

$$= A' j_1(\xi' \frac{r}{a}) e^{-\eta' r/a} \quad r > a$$

where  $\eta' = 3 - \xi'^2 (1 - \xi' \cot \xi')^{-1}$ .

Here the  $\xi$ 's are variational parameters, the  $\eta$ 's are determined from the condition that both the wave function and its radial derivative have to be continuous at  $r = a$ ,  $A$  is a normalisation constant and  $j_n(x)$  is the spherical Bessel function of order  $n$ <sup>(13)</sup>. The optical transition energy of the F-band was then determined from the difference in the energy eigenvalues of the ground and excited states.

For LiF an F-centre transition energy of 4 eV was obtained. This is comparable with Kojima's value of 4.18 eV in the absence of polarisation. Gourary and Adrian found that when applied to the point ion model, polarisation and lattice distortion effects made only very small changes in the transition energy. In fact the neglect of polarisation was found to be negligible for the ground state and to alter the first excited state energy by only about 3%. The influence of lattice distortion changed the transition energy by about 7%. This can be seen to be quite reasonable since in LiF the

wavefunctions are consistent with about 79% of the electronic charge being concentrated inside the vacancy in the ground state and about 51% of the electronic charge being concentrated inside the vacancy for the first excited state. The charge on the vacancy has therefore been effectively screened by the charge cloud associated with the trapped electron. Thus the polarisation is expected to have only a small effect on the transition energy. It is generally recognised that even when polarisation effects are not negligible, they change the excited and ground state energies by roughly the same amount and do not alter the transition energy significantly, nevertheless they will have a very pronounced effect on the binding energy.

### 2.2.3. Ion Size Corrections

The simplicity of the point ion model arises from the neglect of motion of the ion core electrons. In reality the spatial extent of the F-centre electron encloses several shells of ions around the F-centres<sup>(18)</sup> and there is considerable overlap of the appropriate wave functions. To include the finite ion size explicitly in calculations of F-centre properties, requires a many electron calculation in which a determinantal wave function is set up containing the wavefunctions of the trapped electron and all the ion core electrons. Fortunately the compact nature of the trapped electron wave function ensures that only a few shells of ions around

the vacancy need be considered. Kojima's calculations for LiF took account of the nearest and next nearest neighbours. For LiF also Adrian and Gourary<sup>(10)</sup> considered only the nearest neighbour Li<sup>+</sup> ions. They orthogonalised the F-centre envelope function to the Li<sup>+</sup> orbital using the Schmidt process. Thus their F-centre wave function is simply

$$\phi_F = N \left[ \psi_F - \sum_{\alpha} \langle \psi_F | \psi_{\alpha, \text{Li}^+ 1s} \rangle \psi_{\alpha \text{Li}^+ 1s} \right] \quad 2.14$$

This wave function was used with the |1s> orbitals centred on the six nearest Li<sup>+</sup> ions in a determinantal wave function. The total energy was then minimised according to the Hartree-Fock scheme using the determinantal wave function. They neglected all many body forces, i.e. terms involving the F electron and the charge cloud of two or more |1s> orbitals centred on different Li<sup>+</sup> ions. The various two centre integrals were evaluated by expanding the F centre wave function about the Li<sup>+</sup> nucleus taking only the first non-vanishing term in the resulting series. They separated the Hamiltonian into two parts, one due to the point-ion-lattice and the other due to exchange and finite ion size effects. The inclusion of exchange and finite ion size increased the F electron charge distribution inside the vacancy. Although the inclusion of exchange and finite ion size effects changed the ground state energy significantly,

(-0.206 a.u. as compared with the point ion lattice of -0.297 a.u.). Gourary and Adrian<sup>(10)</sup> suggested that the transition energy was not similarly affected. The most significant improvement as a result of these effects was observed in the isotropic hyperfine constant. They obtained a value of only 50 MHz for the nearest neighbour  $\text{Li}^+$  ion as compared with 110 MHz determined using the point-ion-lattice model. The experimentally determined value was 38.5 MHz<sup>(19)</sup>.

The point ion lattice approximation is not particularly well suited to the calculation of hyperfine interaction parameters. This is due to the neglect of an essential ingredient in calculations of the hyperfine interaction constants; the motion of the trapped electron inside the ion cores. All calculations of the hyperfine constants in the point-ion approximation yield values which are several times larger than those determined experimentally. This may be understood qualitatively as follows: The F-electron in a point ion model effectively moves in a lattice of bare nuclei, almost as though the core electrons did not exist. Thus the concentration of the F-centre electron charge cloud at the nucleus is too large. This is also consistent with the reduced magnitude of the hyperfine interaction when exchange and finite ion size corrections are added to the point-ion-lattice approximation, since both interactions effectively repel the F-electron from the neighbouring nuclei.

The above calculations of the ion size effect take into account the detailed motions of the core electrons. For the heavier ions the calculations are increasingly difficult because overlap between different ion cores may not be neglected. In such circumstances the method by Bartram, Stoneham and Gash<sup>(20)</sup> may be more attractive. In the B.S.G. calculation the ion size and exchange effects are contained in two parameters which are calculated explicitly. This calculation is in fact a modification of Gourary and Adrian's point-ion-lattice approximation based on the pseudopotential method of Phillips and Kleinman<sup>(21)</sup> and others<sup>(22)</sup>. The pseudo-potential was optimized to give the smoothest possible pseudo-wave function<sup>(23)</sup>. B.S.G. separate the optimum pseudo-potential into the form,

$$V_P = V_{PI} + (V - V_{PI}) + P(\bar{V} - V) \quad 2.15$$

where  $V_{PI}$  is the point ion potential,  $V$  the true potential,  $P$  the projection operator and  $\bar{V}$  the averaged pseudo-potential. The last two terms in equation (2.15), which represent the difference between the optimum pseudo-potential and the point ion potentials, then constitute the ion size correction to the Hamiltonian. In calculating the expectation value of this pseudo-potential they assumed a tight binding model for the ion core states and neglected the overlaps of ion core orbitals centred on different ions. They approximate further

by neglecting the variation of the pseudo-wave function over each ion core in calculating the expectation value of  $V_P - V_{PI}$ , with the result that the ion size correction is:

$$\langle \phi | V_P | \phi \rangle - \langle \phi | V_{PI} | \phi \rangle = \sum_{\gamma} C_{\gamma} |\phi(r_{\gamma})|^2 \quad 2.16$$

where  $C_{\gamma} = A_{\gamma} + (\bar{V} - U_{\gamma})B_{\gamma}$  2.17

$$A_{\gamma} = \int (1 - P_{\gamma}) (V_{\gamma} - V_{PI\gamma}) d\tau - \int P_{\gamma} V_{PI\gamma} d\tau$$

$$B_{\gamma} = \int P_{\gamma} d\tau, \quad 2.18$$

where  $V_{\gamma}$  is the detailed potential due to the  $\gamma$ th ion,  $U_{\gamma}$  the spherically symmetric part of the point ion potential at the  $\gamma$ th ion; the potential due to the  $\gamma$ th ion itself is not counted. The coefficients  $A_{\gamma}$  and  $B_{\gamma}$ , which are properties of the individual ions, have been computed and tabulated for a large number of ions by B.S.G. Since  $\bar{V}$  appears both on the left and right hand side of equation 2.16 it must be determined self-consistently for each state. They applied the ion size correction not only to the F-band energies in the alkali halides but also to the pressure shifts of the F-band<sup>(25)</sup>. The agreements between calculated and experimental results were rather poor, the computed energies being too small for compounds with large anions and too large for compounds with large cations. In order to improve agreement between theory and experiment it was necessary to diminish all of the  $A_{\gamma}$ 's by the same factor  $\alpha = 0.53$ . When this

correction to  $A_Y$  is introduced the calculated values are in better agreement with experiment and with the Mollwo-Ivey law<sup>(26)</sup> than are the point ion calculations of Gourary and Adrian. The theory also accounts for the F-band energies for a number of salts which depart from the Mollwo-Ivey law. A complete comparison between theory and experiment is shown in Table 2.

B.S.G. further applied their theory to the F-bands of the alkaline earth fluorides  $\text{CaF}_2$ ,  $\text{SrF}_2$  and  $\text{BaF}_2$ . The method used was essentially the same as for the alkali halides. Again when the values of  $A_Y$  for all the ions were reduced by  $\alpha = 0.53$ . they obtained a considerable improvement over the point-ion results. Taken together, these two sets of results suggest the definition of a set of pseudo-potential coefficients in which the reduction of the  $A_Y$  by the factor of 0.53 is tolerably well justified.

### 2.3. F<sup>+</sup>-centres in Alkaline Earth Oxides

The F<sup>+</sup>-band for the four oxides, MgO, CaO, SrO and BaO have been identified experimentally using the techniques of optical absorption and paramagnetic Faraday rotation. The peak positions for the F<sup>+</sup>-bands occur at 4.95 ev, 3.7 ev, 3.0 ev and 2.0 ev in the series MgO, CaO, SrO and BaO. Kemp and Neeley's<sup>(14)</sup> calculations indicate that given suitable wave functions one might obtain good agreement with the experimental results using the point-ion-lattice approximation. These authors neglected ion size effects

and it is of importance to determine whether such effects are as important to the oxides containing heavy cations as they are to the alkali halide and alkaline earth fluorides. Furthermore it appears that the BaO  $F^+$ -band occurs at a much lower photon energy than might be expected and one might hope to effect an improvement in the theoretical value using similar methods to those used by Bartram, Stoneham and Gash<sup>(20)</sup>. In this section, we review first of all Kemp and Neeley's calculations and thus our own calculations on the alkaline earth oxides.

### 2.3.1. Kemp and Neeley's Calculations on Oxides

Kemp and Neeley<sup>(14)</sup> treated the  $F^+$ -centre in magnesium oxide using a linear combination of atomic orbital wave function with a point-ion-lattice Hamiltonian. Their L.C.A.O. wave functions, which were composed of  $|3s\rangle$  and  $|3p\rangle$  wave functions centred on the nearest neighbour cations, were then expanded about the vacancy centre using Löwdins  $\alpha$ -function<sup>(15)</sup>. In the actual calculation the wave functions were approximated by a single spherical harmonic term corresponding to the lowest value of  $l$  appropriate to the function expressed in cubic harmonics. The simplified point-ion-lattice Hamiltonian which contained only the lowest  $l$  terms in the point-ion potential then had the form,

$$H = -\frac{1}{2r^2} \frac{d}{dr} \left( r^2 \frac{d}{dr} \right) + \frac{l(l+1)}{2r^2} + V_0(V) \quad 2.19$$

The L.C.A.O. wave function and their expansion now takes the form:

$$\begin{aligned} \psi_{im}^j &= d_{im}^j \sum_{\mu}^S \phi_{\mu} = C_{im}^j \alpha_{\ell} (NLM|a,r) Y_{em}(\theta, \phi) \\ &= \tilde{\psi}_{im}^j \end{aligned} \quad 2.20$$

Where  $\psi_{im}^j$  is the mth L.C.A.O. belonging to the jth row of the ith irreducible representation  $\Gamma_i^P$  of  $O_h$  symmetry.  $\tilde{\psi}_{im}^j$  is the truncated wave function containing only the lowest value of l in the expansion,  $d_{im}^j$  and  $C_{im}^j$  are normalisation constants, and  $\mu$  runs over the particular set of S single ion functions  $\phi_{\mu}$  involved in the L.C.A.O. The relationship between  $d_{im}^j$  and  $C_{im}^j$  was determined by adopting Löwdin's normalisation procedure for the  $\alpha$ -function and the spherical harmonics. Using symmetry arguments they were able to determine the expansion of the various ground and excited L.C.A.O. in terms of the  $\alpha$ -function. For simplicity Löwdin's  $\alpha$ -functions were calculated using Slater orbitals.

They solved the secular equations using their lowest l wave function expansion for ground and excited states, and obtained the results for the energy eigenvalues shown in Table (1). The corresponding eigenfunctions for the ground ( $\Gamma_1$ ) and excited ( $\Gamma_4'$ ) states were,

$$\begin{aligned} \Gamma_1 \quad \psi_{00}^0 &= 0.396 \tilde{\psi}_{01}^0 + .710 \tilde{\psi}_{02}^0 \\ \Gamma_4' \quad \psi_{10}^0 &= -0.355 \tilde{\psi}_{11} - .577 \tilde{\psi}_{12}' + 1.186 \tilde{\psi}_{13}' \end{aligned} \quad 2.21$$

The strong p-character in the ground state is seen in the  $\tilde{\psi}_{02}^0$  term, which consists of the 3p orbitals of the surrounding 6  $\text{Mg}^{1+}$  ions. This compares with Kojima's L.C.A.O. calculation<sup>(9)</sup> which also contained a large contribution of p-wave function in the ground state. In the L.C.A.O. scheme p-like character in the ground state may be partly explained by the electron being regarded as equally shared among the six surrounding cations. Consequently the ground state is not spherically symmetric, as is usually assumed in point ion model<sup>(10)</sup>.

Following Gourary and Adrian<sup>(10)</sup>, Kemp and Neeley<sup>(14)</sup> applied the ion core polarisation and distortion corrections to their results. They argued that the polarisation correction to the energy due to the ions other than the six nearest neighbour cations and twelve nearest neighbour anions were not important because the interaction of a charge with a polarisable ion decreases as  $r^{-4}$ . They treated therefore the polarisation of the six  $\text{Mg}^{2+}$  ions and the  $12\text{O}^{2-}$  ions and the displacements of the six  $\text{Mg}^{2+}$  ions only. The results of their calculations are also shown in Table (1). The agreement with experiment is quite good.

Kemp<sup>(16)</sup> later reported similar theoretical results for calcium oxide strontium oxide and barium oxide. The estimated positions of the  $F^+$ -bands, when taken with the value for magnesium oxide, must be regarded as in good agreement with experiment except

for barium oxide. The poor result for barium oxide is presumably due to errors in the polarisation and distortion corrections and to neglect of ion size effects. This latter neglect may be crucial since it has been shown to be important in alkali halides containing of heavy cation and in barium fluoride<sup>(17)</sup>.

Neeley<sup>(18)</sup> complemented this initial study using a slightly different approach in which he assumed the ground and excited state wave function to be gaussian functions. The gaussian function was chosen because of its simplicity but especially because of its rapid convergence in calculating lattice sums. The results of his calculations are also shown in Table 1.

### 2.3.2. Extension of the Point Ion Lattice Calculation

We first calculate the binding and transition energies of the  $F^+$ -centres in these four oxides within the framework of the point-ion-lattice model using wave functions which are different to those used by Kemp and Neeley<sup>(14)</sup>. We later include polarisation and lattice distortion effects which are especially important for the  $F^+$ -centres because of their effective positive charge. There is no rigorous way of taking the ion core polarisation effects into account except by a complete solution of the many electron problem. Therefore in including the polarisation and lattice distortion corrections to the point-ion-lattice approximations we assume

1. that the Born model of ionic solids applies to the alkaline earth oxides, and
2. that the polarisation of the cations and anions can be represented by induced point dipoles.

Later we also calculate the ion size effects on the transition and binding energy of the  $F^+$ -centre in the four oxides, using the pseudo-potential method of Bartram, Stoneham and Gash<sup>(20)</sup>.

In the point-ion-lattice approximation each ion is represented by a point charge of magnitude equal to the valency of the ion which it represents. The most important interaction between the trapped electron and the ions is the classical Coulomb interaction. In a cartesian co-ordinate system the centre of which is at the centre of the  $F^+$ -centre, the coulomb energy of the defect electron in the field of all the ions regarded as point charges is given by

$$V_L(r) = Z \sum_i (-1)^{x_i+y_i+z_i} \{ (x-x_i)^2 + (y-y_i)^2 + (z-z_i)^2 \}^{-\frac{1}{2}} \quad (2.22)$$

where  $(x_i, y_i, z_i)$  are the Cartesian co-ordinates of the  $i^{\text{th}}$  ion from the centre of the vacancy, and  $Z$  is the valency of the ion. In the absence of interactions apart from this we can write the simplified point-ion Hamiltonian,

$$H = T + V_L(r)$$

For crystals with the NaCl structure, Gourary and Adrian expanded the potential energy  $V_L(r)$  in terms of cubic harmonics,

$$V_L(r) = V_{00}(r)Q(\Gamma_1^{\ell}, 0, 0 | \theta, \phi) + V_{40}(r)Q(\Gamma_1^{\ell}, 4, 0 | \theta, \phi) \quad 2.24$$

where the cubic harmonic is defined by,

$$Q(\Gamma_i^P, \ell, \mu_{\ell} | Q, \phi) = \sum_{m=-\ell}^{+\ell} C(\Gamma_i^P, \ell, \mu_{\ell}, m) Y_{\ell m}(\theta, \phi), \quad 2.25$$

and  $\Gamma_i^P$  is the  $i$ th irreducible representation of the cubic group  $O_h$ ,  $\mu_{\ell}$  an index used to differentiate among several  $Q$ 's of the same  $\ell$  belonging to the same  $\Gamma_i^P$ , and  $Y_{\ell m}$  are the usual spherical harmonics.

The individual  $V_{\ell, \mu_{\ell}}(r)$ 's are determined by expanding each term in the potential about the centre of the vacancy. Since  $V_L(r)$  has the symmetry of the full cubic group the solution to our equation must also belong to an irreducible representation of the cubic group. Thus

$$\psi(\Gamma_i^P | r) = \sum_{\ell=0}^{\infty} \sum_{\mu_{\ell}} R(\Gamma_i^P, \ell, \mu_{\ell} | r) Q(\Gamma_i^P, \ell, \mu_{\ell} | \theta, \phi) \quad 2.26$$

In general we only keep the first term in this expansion, i.e. we put

$$\psi(\Gamma_i^P | r) = R(\Gamma_i^P, \ell, \mu_{\ell} | r) Q(\Gamma_i^P, \ell, \mu_{\ell} | \theta, \phi)$$

In our case we consider only the ground and first excited states of the  $F^+$ -centre which we assume to be s-like and p-like respectively. The following functions were then chosen as the normalised trial wave

functions for the ground and excited states:

Ground State:

$$\begin{aligned}
 Q(\Gamma_{1,0,0}^{\ell} | r) &= (4\pi)^{-1/2} \\
 R(\Gamma_{1,0,0}^{\ell} | r) &= \frac{\sqrt{4\alpha^3}}{7} (1 + \alpha r) e^{-\alpha r}
 \end{aligned}
 \tag{2.27}$$

Excited State:

$$\begin{aligned}
 Q(\Gamma_{4,1,0}^o | r) &= \frac{\sqrt{3}}{4\pi} \cos \theta \\
 R(\Gamma_{4,1,0}^o | r) &= \frac{\sqrt{4\beta^5}}{3} r e^{-\beta r}
 \end{aligned}
 \tag{2.28}$$

$\alpha$  and  $\beta$  are variational parameters.

Therefore we may put

$$\psi_s = \frac{\sqrt{\alpha^3}}{7\pi} (1 + \alpha r) e^{-\alpha r}
 \tag{2.29}$$

$$\psi_p = \frac{\sqrt{\beta^5}}{\pi} r e^{-\beta r} \cos \theta
 \tag{2.30}$$

for our ground and excited state wave functions respectively. Our problem is therefore the determination of the variational parameters  $\alpha$  and  $\beta$  such that the energy functionals

$$E_n = \int \psi_n(r) [-\nabla^2 + 2V_L(r)] \psi_n(r) d\tau
 \tag{2.31}$$

are minimised, where  $n$  stands for  $s$  or  $p$  as the case may be. Using these wavefunctions, the energy functionals (in Rydberg units) are found to be, as shown in the appendix;

$$E_s = \frac{3\alpha^2}{7} - \frac{4\alpha_M}{a} - \frac{2}{7} \sum \frac{(-1)^{N_i} M_i}{R_i} (2\alpha^3 R_i^3 + 10\alpha^2 R_i^2 + 19\alpha R_i + 14) e^{-2\alpha R_i} \quad 2.32$$

$$E_p = \beta^2 - \frac{4\alpha_M}{a} - \frac{2}{3} \sum \frac{(-1)^{N_i} M_i}{R_i} (2\beta^3 R_i^3 + 6\beta^2 R_i^2 + 9\beta R_i + 6) e^{-2\beta R_i} \quad 2.33$$

The first terms in Equations 2.32 and 2.33 are the kinetic energy of the electron in the ground state ( $E_s$ ) and the first excited state ( $E_p$ ) and  $\alpha_M = 1.74756$  is the Madelung's constant for crystals of the NaCl structure. The summations are to be taken over different shells centred on the vacancy and  $M_i$  is the number of ions in the  $i$ th shell and  $N_i$  is odd or even according as the  $i$ th shell is occupied by cations or anions. These energy functionals are to be minimised with respect to  $\alpha$  or  $\beta$ . The final results give the transition energy and the binding energy of the ground state and the excited state. The resulting energies are tabulated together with the experimental results in Table 3.

It is seen that the deviation of the calculated results from the experimental results increases along the series from MgO to BaO. For MgO which is the least polarisable of the four oxides, the agreement between the calculated and the experimental results is the best. For BaO which has the highest polarisability the agreement is rather poor. It is therefore reasonable to suppose that the polarisation effect plays a very important role in these oxides, although in the

heavier oxides such as BaO the effects of the partial covalent binding may be important.

### 2.3.3 Polarisation and Lattice Distortion Corrections

As we mention above the polarisation effects are expected to have an important bearing on the  $F^+$ -centre transition energies in the alkaline earth oxides. The ions centred on the vacancy are not only polarised by the net charge of the vacancy but are also displaced to a new equilibrium position. We now calculate the effects which polarisation and distortion have on the transition and binding energies of the  $F^+$ -centre.

We assume that the Frank-Condon's principle applies for the first transition energy. We assume further that the core electrons respond only to the average position of the defect electron, i.e. the Hartree-Fock's procedure applies. If  $\Delta W_t$  is the total change of energies of the system, then

$$\Delta W_t = \Delta W_e + \Delta W_L + \Delta W_p \quad 2.34$$

where  $\Delta W_e$  is the change of energy of the  $F^+$ -electron due to the lattice distortion,  $\Delta W_L$  is the change of energies of the lattice due to the same distortion and  $\Delta W_p$  is the interaction of the lattice distortion with the induced polarisation.

We allow only the nearest neighbour cations to move their new equilibrium position  $(1 + \sigma)a$ , here  $\sigma$  is positive when the

distortion is in a direction away from the centre of the vacancy. Following Kemp and Neeley<sup>(14)</sup> we consider the polarisation of the nearest cations and the nearest anions only. Our problem is therefore to find the new equilibrium position  $\sigma_0$  subject to the condition that the total energies of the system, electron plus lattice, is a minimum at this position. The change of  $F^+$ -electron energy may be easily calculated by expanding the part of the electron energy due to the six distorted cations. This part of the energy is,

$$\Delta W_e = \left[ \frac{24}{a} - 6 X' \right] \sigma + \left[ -\frac{24}{a} + 3 X'' \right] \sigma^2, \quad 2.35$$

where 
$$X' = \frac{2}{7a} (4\alpha^4 a^4 + 16\alpha^3 a^3 + 28\alpha^2 a^2 + 28\alpha a + 14)e^{-2\alpha a} \quad 2.36$$

$$X'' = \frac{2}{7a} (8\alpha^5 a^5 + 24\alpha^4 a^4 + 40\alpha^3 a^3 + 56\alpha^2 a^2 + 56\alpha a + 28)e^{-2\alpha a} \quad 2.37$$

and  $a$  is the lattice parameter.

Our calculation of the lattice energy change follows closely that of Gourary and Adrian. Assuming a repulsive interaction of the form  $br^{-\lambda}$  the total change of the lattice energy is simply

$$\Delta W_L = \left( \frac{8\alpha_M}{a} - \frac{48}{a} \right) \sigma + \left( \frac{4\alpha_M (\lambda-3)}{a} + \frac{104.912}{a} \right) \sigma^2 \quad 2.38$$

Next we calculate the interaction of the lattice distortion with polarisation. This term arises from the fact that a distortion of the cation will necessarily have to do work against the dipole fields. Therefore we have to calculate the induced dipoles on the six nearest cations and twelve nearest anions. The total field acting on a lattice site consists of the following parts:

1. The field due to the vacancy plus the part of the  $F^+$ -electron charge cloud trapped inside the vacancy,
2. The field due to the displacement of the six cations and
3. The field due to the other induced dipoles.

In general the dipolar field has the effect of reducing the total field acting on a lattice site. This field is called the depolarising field. For a highly symmetrical system the effect of this field is to lower the total polarising field by a factor depending only on the geometrical arrangement of the dipoles. Therefore this part of the field may be taken into account by simply multiplying the total polarising field by the "depolarising factor". For a general discussion of calculating the induced dipole moments we refer to Chapter 5 where we shall discuss the effect of polarisation on the  $F_C^+$ -centre energies. Here we only quote the result given in Neeley's thesis<sup>(15)</sup>.

If the induced dipole moment on the nearest neighbour cations is  $p^+$  pointing in the radial direction, then

$$P^+ = \alpha^+ k^+ \left[ F_q + F_{\text{dist.}} + F(P^-)_{\text{dip-dip}} \right] \quad 2.39$$

where  $k^+$  is the depolarisation factor for the six nearest neighbour cations

$$k^+ = \beta \left[ 1 + (1-\beta) 3\sigma + (1-4\beta + 3\beta^2) 3\sigma^2 \right] \quad 2.40$$

$$\beta = 1 / \left[ 1 + 2.732 \frac{\alpha^+}{a} \right]$$

$F_q$  is the field at the cation due to the excess charge of the centre

$$F_q = e (2 - \epsilon^+) / \left[ a(1 + \sigma) \right]^2 \quad 2.41$$

$F_{\text{dist}}$  is the field at a cation due to the other five distorted cations and is given by

$$F_{\text{dist}} = \frac{1}{a^2} \left[ -4.742 \sigma + 10.294 \sigma^2 \right] \quad 2.42$$

$F(p^-)_{\text{dip-dip}}$  is a dipole field at a cation due to the twelve anion dipoles. This field consists of a geometrical factor times the dipole field of an anion  $p^-$

$$f(\sigma) = \frac{1}{a^2} (4.573 + 6.999\sigma - 12.831 \sigma^2) \quad 2.43$$

$$F(p^-)_{\text{dip-dip}} = f(\sigma)p^-$$

Similarly the induced dipole moment on the nearest neighbour anions can be expressed as

$$p^- = \alpha^- k^- \left[ E_q + E_{\text{dist}} + E(p^+)_{\text{dip-dip}} \right] \quad 2.44$$

The symbol E stands for the field acting on an anion and the various terms in this equation have the corresponding meaning for those appeared in  $p^+$ . Hence

$$k^- = 1/(1 + 2.707 \frac{\alpha^-}{a}) \quad 2.45$$

$$E_q = e(2-\epsilon^-)/2a^2 \quad 2.46$$

$$E_{\text{dist}} = \frac{1}{a^2} (-4.58 \sigma - 3.51 \sigma^2) \quad 2.47$$

$$h(\sigma) = \frac{1}{a^3} (2.286 + 3.50 \sigma - 6.415 \sigma^2) \quad 2.48$$

$$E(p^+)_{\text{dip-dip}} = h(\sigma)p^+$$

Therefore by combining the above equations, we have the induced dipole moment on an anion

$$P^- = \alpha^- k^- \left[ E_q + E_{\text{dist}} + \alpha^+ k^+ h(\sigma) (F_q + F_{\text{dist}}) \right] / \left[ 1 - \alpha^- \alpha^+ k^- k^+ h(\sigma) f(\sigma) \right] \quad 2.49$$

and that on a cation

$$P^+ = \alpha^+ k^+ \left[ F_q + F_{\text{dist}} + \alpha^- k^- h(\sigma) (E_q + E_{\text{dist}}) \right] / \left[ 1 - \alpha^- \alpha^+ k^- k^+ h(\sigma) f(\sigma) \right] \quad 2.50$$

We then expand  $p^-$  and  $p^+$  to the second order in  $\sigma$ . The expressions are rather tedious to write out; in general it can be shown that,

$$p^- = \alpha^- k^- (A_0 + A'\sigma + A''\sigma^2) \quad 2.51$$

$$p^+ = \alpha^+ k^+ (B_0 + B'\sigma + B''\sigma^2) \quad 2.52$$

The polarisation distortion interaction consists of the following two parts:

1. the work done against the dipole field in moving the charge of the six cation a distance  $\sigma$  and
2. the work done in moving the induced dipole on the six cations against all fields through the same distance.

The field acting on one of the six cations due to the induced dipoles on the twelve anions is

$$\begin{aligned} F_p &= \alpha^- k^- (E_q + E_{\text{dist}}) f(\sigma) \\ &= \frac{\alpha^- k^-}{a^2} \left[ 4.573 E_q + \frac{(-20.94 + 6.999 E_q)}{a^2} \sigma \right] \quad 2.53 \end{aligned}$$

and the work done is therefore

$$\begin{aligned} \Delta W(\sigma)_1 &= 12 q a \int_0^\sigma F_p d\sigma \\ &= \frac{24 \alpha^- k^-}{a^2} \left[ 4.573 E_q \sigma + \frac{1}{2} \frac{(-20.94 + 6.999 E_q)}{a^2} \sigma^2 \right] \quad 2.54 \end{aligned}$$

where  $q$  is the charge of the cation.

Next we calculate the work done against all fields in moving the dipole on the six cations a distance  $\sigma$ . According to elementary electrostatics the force acting on a dipole due to the field  $E$  is,

$$\vec{F} = (\vec{P} \cdot \nabla) \cdot \vec{E} = \frac{1}{\alpha^+} (\vec{P} \cdot \nabla) \cdot \vec{P} \quad 2.55$$

Since in our case the dipoles are assumed to be pointing radially outwards from the vacancy centre, the force is simply,

$$\vec{F} = \frac{1}{2\alpha^+ a} \frac{\partial}{\partial \sigma} (P^+{}^2), \quad 2.56$$

and the work done,

$$\begin{aligned} \Delta W(\sigma)_2 &= \frac{12}{2\alpha^+} \int_0^\sigma \frac{d}{d\sigma} (P^+{}^2) d\sigma \\ &= 6\alpha^+ k^+{}^2 \left[ 2B_{\circ} B' \sigma + (2B_{\circ} B'' + B''^2) \sigma^2 \right] \quad 2.57 \end{aligned}$$

The total polarisation distortion interaction is the sum,

$$\Delta W_p = \Delta W(\sigma)_1 + \Delta W(\sigma)_2$$

The total change of energy of the system which, is the sum of  $\Delta W_e$ ,  $\Delta W_L$  and  $\Delta W_p$ , is then minimised with respect to  $\sigma$ .

The expectation value of the energy of the electron in the field of the point dipoles is

$$\begin{aligned} \Delta E &= -2 \cdot \vec{P} \cdot \vec{E} \\ &= -24 p^- \frac{(\partial I_s)}{\partial R} \frac{1}{\sqrt{2a}} - 12 p^+ \frac{(\partial I_s)}{\partial R} a, \end{aligned} \quad 2.59$$

where

$$\frac{\partial I_s}{\partial R} = \frac{1}{R^2} - \frac{1}{14R^2} (4\alpha^4 R^4 + 16\alpha^3 R^3 + 28\alpha^2 R^2 + 28\alpha R + 14)e^{-2\alpha R} \quad 2.60$$

is the electrostatic field of the defect electron. The subscript stands for the lattice site where the electric field is to be evaluated.

Similarly the correction to the excited state is given by replacing

$\frac{\partial I_s}{\partial R}$  by  $\frac{\partial I_p}{\partial R}$  where

$$\frac{\partial I_p}{\partial R} = -\frac{1}{R^2} + \frac{1}{6R^2} (4\beta^4 R^4 + 8\beta^3 R^3 + 12\beta^2 R^2 + 12\beta R + 6)e^{-2\beta R} \quad 2.61$$

and  $p^-$  and  $p^+$  are to be replaced by that corresponding to the excited state, that is the  $\epsilon^+$  which appears in  $F_q$  and  $E_q$  is to be replaced by the  $\epsilon^-$ , where  $\epsilon^-$  is the part of the excited state charge cloud trapped inside the vacancy. This is given by

$$\epsilon^- = 1 - (1 + 2\beta R + 2\beta^2 R^2 + \frac{4}{3} \beta^3 R^3 + \frac{2}{3} \beta^4 R^4) e^{-2\beta R} \quad 2.62$$

The results of the calculation after polarisation and distortion correction is also shown in Table 3. We see a marked improvement of the agreement between the calculated results and the experiment. The general trend of the decrease of the  $F^+$ -band energy from MgO to BaO is clearly seen to be in qualitative agreement with the experiment. A least square fit of the calculated results for the four oxides gives the following Ivey relation,

$$\Delta E = 64.957 a^{-1.888} \text{ ev} \quad 2.63$$

The percentage error is less than 0.1% for the four oxides. A similar least square fit for the experimental results gives,

$$\Delta E = 429.059 a^{-3.191} \text{ ev} \quad 2.64$$

The percentage error is within 6% to 8% for the three oxides MgO, CaO and SrO while it is 10% for the BaO. If we regard the deviation from the Ivey's law as an indication of the ion size effect, it clearly indicates the increasing importance of the ion size effect from MgO to BaO.

#### 2.3.4. Ion Size Correction for the Alkaline Earth Oxides

Although polarisation and lattice distortion corrections to the point ion lattice model give good results for MgO and CaO, they fail to account for the small  $F^+$ -band energies in SrO and BaO. It is certainly arguable whether the latter two oxides can still be treated

as purely ionic solids within Born's model. However one might expect that the finite ion size effects would be able to explain, at least partially, the discrepancy between theory and experiment. In the absence of simpler procedures for taking ion size effects into account, we have adopted B.S.G.'s pseudopotential method for  $F^+$ -centre in the alkaline earth oxides.

According to Equ. (2.16), the potential energy of the trapped electron in the pseudopotential scheme is

$$\bar{V}_P = \bar{V}_{PI} + \sum_{\gamma} M \{ A_{\gamma} + (\bar{V}_P - U_{\gamma}) B_{\gamma} \} |\phi(r_{\gamma})|^2 \quad 2.65$$

where  $\phi(r_{\gamma}) = \psi_s(r_{\gamma})$  for the ground state and  $\phi(r_{\gamma}) = \psi_p(r_{\gamma})$  for the excited state.  $A_{\gamma}$  and  $B_{\gamma}$  are the pseudopotential coefficients which incorporate the ion size effects. These coefficients have been tabulated by B.S.G. for numerous ions: only those appropriate to the alkaline earth oxides are given in Table 4.

The spherically symmetric part of the potential  $U_{\gamma}$  is given in Rydberg units by,

$$U_{\gamma} = -\frac{4\alpha_M}{a} - (-1)^{N_{\gamma}} \frac{4}{r_{\gamma}} \quad 2.66$$

where  $N_{\gamma}$  is odd or even according to whether the  $\gamma$ th ion is the metal ion or the oxygen ion. Therefore the total energy of the electrons is

(i) in the ground state

$$H_s = E_s + \frac{\alpha^3}{7\pi} \sum_{\gamma} M \{ A_{\gamma} + (\bar{V}_s - U_{\gamma}) B_{\gamma} \} (1 + \alpha r_{\gamma})^2 e^{-2\alpha r_{\gamma}} \quad 2.67$$

and (ii) in the excited state,

$$\begin{aligned}
 H_p &= E_p + \frac{\beta^5}{\pi} \sum_Y \{A_Y + (\bar{V}_p - U_Y)B_Y\} r_Y^2 e^{-2\beta r_Y} \text{Cos}^2 \theta_Y \\
 &= E_p + \frac{\beta^5}{3\pi} \sum_Y M_Y \{A_Y + (\bar{V}_p - U_Y)B_Y\} r_Y^2 e^{-2\beta r_Y} \quad 2.68
 \end{aligned}$$

where  $E_s$  and  $E_p$  are given by Equ. (2.32) and Equ. (2.33) and for  $H_p$  we have made use of the easily demonstrable fact that the summation of  $\text{Cos}^2 \theta$  over each shell is equal to 1/3 times the spherically symmetrical part of the summation. Equ. (2.67) and Equ. (2.68) are to be minimised with respect to  $\alpha$  and  $\beta$  respectively and at the same time solved self-consistently with respect to the pseudopotential  $\bar{V}$ .

Our problem is therefore (i) to solve the equations (2.67) and (2.68) self-consistently with respect to the pseudopotential  $\bar{V}_i$ , where  $i$  stands for  $s$  or  $p$  as the case may be, and (ii) to find the variation parameter  $\alpha$  ( $\beta$ ) such that  $H_s$  ( $H_p$ ) is minimised. For simplicity, we shall give the detail calculations for  $E_s$  only. The calculations for  $E_p$  proceed along similar lines.

We can either (i) with a suitably chosen  $\alpha$ , solve Equ. (2.67) self-consistently with respect to  $V_s$  and then with the self-consistent  $V_s$  minimise  $H_s$  with respect to  $\alpha$  or (ii) with every suitably chosen  $\bar{V}_s$  minimise  $H_s$  with respect to  $\alpha$  until self-consistency of  $\bar{V}_s$  is obtained. We have followed the first procedure in our calculations. In order to start the self-consistent calculation and the minimisation of  $H_s$  using

numerical methods, it is essential to start with a suitably chosen value of  $\alpha$  and  $\bar{V}_S$ . We have chosen the point ion values of  $\alpha$  and  $\bar{V}_S$  for a start. The calculation therefore consists of the following three steps:

- (i) From the point ion calculation, we set  $\alpha = \alpha'$  and  $\bar{V}_S = \bar{V}_S(1) = E_S' - 3\alpha'^2/7$ , where the superscript refers to the values obtained from a point ion calculation;  $\bar{V}_S(1)$  means the starting value of the pseudopotential. For the purpose of using the Newton-Raphson<sup>(27)</sup> method to minimise the total energy, it is also necessary to set the derivatives of  $\bar{V}_S(1)$  with respect to  $\alpha$  equal to its counterpart in a point ion calculation.
- (ii)  $H_S$  is calculated using Equ. (2.67) with  $\alpha$  and  $\bar{V}_S$  as given in (i). We assume that the result of this calculation gives a pseudopotential  $\bar{V}_S(2)$  which is equal to the total energy minus the kinetic energy.  $\bar{V}_S(2)$  is then compared with  $\bar{V}_S(1)$ . Self-consistency requires that  $\bar{V}_S(2) = \bar{V}_S(1)$ . In actual fact they would never exactly equal and so we should have some criteria as to what degree of self-consistency will satisfy our purpose in hand. If  $|\bar{V}_S(2) - \bar{V}_S(1)|$  did not satisfy our self-consistency requirements then we should go back to the beginning of this step and do the calculation again but this time use  $\bar{V}_S(2)$  in place of  $\bar{V}_S(1)$  as the new  $\bar{V}_S$  in Equ. (2.67), while  $\alpha$  is unchanged. In general if we set the result of the Nth calculation

as  $\bar{V}_s(N)$ , then our criteria for self-consistency requires that

$$|\bar{V}_s(N + 1) - \bar{V}_s(N)| < .001 \quad 2.69$$

A better condition would be

$$\frac{|\bar{V}_s(N + 1) - \bar{V}_s(N)|}{V_s(N)} < .001 \quad 2.70$$

but for our purpose Equ. (2.69) is found to be quite satisfactory.

So if after the Nth repeat of (ii) the self-consistency condition of Equ. (2.69) is satisfied, we then proceed to step (iii).

(iii) This step consists essentially of a numerical solution of a non-linear algebraic equation using the Newton-Raphson method. To minimise  $H_s$  with respect to  $\alpha$  is equivalent to finding the roots of its first derivative with respect to  $\alpha$ . This objective is conveniently achieved by using the Newton-Raphson's numerical method. Here we also need a criteria to decide how accurate the  $\alpha$  should be that will satisfy our purpose. For our case Equ. (2.69) serves also our purpose, i.e. we require that the difference between the Mth calculated results of the first derivative of  $H_s$  with respect to  $\alpha$  and the (M + 1)th calculation should not be more than .001, i.e.

$$|E_s'(M + 1) - E_s'(M)| < .001 \quad 2.71$$

if not, then we have to change the value of  $\alpha$  according to the

Newton-Raphsons formula as is given in all standard textbooks of calculus. The new value of  $\alpha$  is then used in step (i) instead of the previous point ion value. Of course the value of  $\bar{V}_g$  and its derivatives should be changed accordingly, and the whole process from step (i) to step (iii) is repeated until condition (2.71) is satisfied.

A similar calculation is done for  $E_p$ . The results are shown in Table 4. The agreement between the calculated results and the experimental results are seen to be very poor. Although we have used the diminished coefficient  $A_\gamma$  of B.S.G., the calculated results are still too large. While the general trend of the ground state energy from MgO to BaO seems quite reasonable, the excited state energies remain stationary round 8 ev.

The effect of polarisation and lattice distortion may be calculated in the same way as we did in section 2.3.3. The results are also shown in Table 4. It is seen that the agreement between the calculated results and the experiments is less good than before, it is evident that this poor agreement results from a too large correction to the excited state.

References

1. N.F. Mott and M.J. Littleton, *Trans. Far. Soc.* 34, 485, (1938).
2. S.R. Tibbs, *Trans. Far. Soc.* 35, 1471, (1939).
3. J.H. Simpson, *Proc. Roy. Soc.* A197, 269, (1949), *Rbst.* 20  
Int. Conf. Colour Centres in Alkali Halides, Corvallis, (1959).
4. J. Krumhansl and N. Schwartz, *Phys. Rev.* 89, 1154, (1953).
5. M. Born and J.R. Oppenheimer, *Ann. Physik*, 84, 457, (1927).
6. There are many excellent papers and reviews on this subject, see for example:  
J.J. Markham, *Rev. Mod. Physics*, 31, 956, (1959).  
D.L. Dexter, *Solid State Physics*, 6, (Academic Press, 1958).  
K. Huang and A. Rhys, *Proc. Roy. Soc.* A204, 406, (1950).  
S.I. Pekar, *J. Exp. Theoret. Physics (U.S.S.R.)* 20, 510, (1950)  
and 22, 641, (1952).  
W.B. Fowler (Ed) "The Physics of Colour Centres" (Academic Press, 1968).
7. See for example C.C. Klick and J.H. Schulman, *Solid State Physics* 5, (Academic Press, 1957).
8. T. Inui and Y. Uemura, *Prog. Theor. Phys. Jap.* 5, 252, (1950).
9. T. Kojima, *J. Phys. Soc. Jap.* 12, 908 and 918, (1957).
10. B.S. Gourary and F.J. Adrian, *Phys. Rev.* 105, 1180, (1957)  
and *Solid State Physics*, 10, (Academic Press, 1960).

11. See for example R. Courant and D. Hilbert, *Methods of Mathematical Physics*, Vol. I, Interscience Publishers Inc.
12. H.A. Bethe and F.C. Von der Lage, *Phys. Rev.* 71, 612, (1947).
13. See for example *Handbook of Mathematical Functions*, edited by Abramowitz and Stegan, Dover Pub.
14. J.C. Kemp and V.I. Neeley, *Phys. Rev.* 132, 215, (1963).
15. Löwdin, *Advances in Physics*, Vol. 5, No. 17, (1956).
16. J.C. Kemp, *Bull. Amer. Phys. Soc.* 8, 484, (1963).
17. V.I. Neeley, Ph.D. Thesis, Univ. of Oregon, Eugene (1964).
18. See for example Seidel and Wolff, "The Physics of Colour Centres".
19. N.W. Lord, *Phys. Rev. Letters*, 1, 170, (1958).
20. R.H. Bartram, A.M. Stoneham and P. Gash, *Phys. Rev.* 176, 1014, (1968).
21. J.C. Philips and L. Kleinman, *Phys. Rev.* 116, 287, (1959).
22. M.H. Cohen and V. Heine, *Phys. Rev.*, 122, 1821, (1961). See also Ref. 24.
23. W.A. Harrison, *Pseudo-potentials in the Theory of Metals*, Benjamin, (1966).
24. B.J. Austin, V. Heine and L.J. Sham, *Phys. Rev.*, 127, 276, (1962).
25. C.J. Buchenauer and D.B. Fitchen, *Phys. Rev.*, 167, 846, (1968).
26. H.F. Ivey, *Phys. Rev.*, 72, 341, (1947).
27. See for example H. Margenau and G.M. Murphy, "The Mathematics of Physics and Chemistry".

CHAPTER III

EXPERIMENTAL EVIDENCES FOR THE  $F_C^+$ -CENTRE

3.1 E.S.R. Studies of Annealed Crystals

In their pioneering studies of defects in the II-VI compounds Wertz and his associates<sup>(1)</sup> reported changes in the ESR spectra consequent upon thermal bleaching subsequent to reactor irradiation. Their early studies were carried out (where possible) using polycrystalline samples of oxides, sulphides and selenides of Mg, Ca, Sr and Ba, although for MgO single crystals were also used. The changes observed may be summarised as:

- (i) reduced amplitudes in the  $F^+$ -centre ESR spectra,
- (ii) the growth of a new line in the ESR spectrum at the expense of the  $F^+$ -centre spectrum,
- (iii) the line was asymmetric in shape, such that the maximum slope occurred on the high field side of the line,
- (iv) the new line was shifted to higher fields (lower g-value) relative to the  $F^+$ -centre resonance,
- (v) the intensity of the optical band at 4.90 eV decreased in parallel with the  $F^+$ -centre ESR spectrum. This led to the first hint at an assignment for the  $F^+$ -band. Furthermore in MgO single crystals the line width  $\Delta H$  varied with orientation such that  $\Delta H_{100}/\Delta H_{110} = \frac{1}{2}$ .

Wertz et al, proposed that these observations were consistent with the formation of defects which consisted of single electrons trapped at cation-anion vacancy pairs,  $F_C^+$ -centres in our notation. Wertz et al<sup>(1)</sup> reported the g-values of the centres for the alkaline earth oxides and also MgS, SrS, MgSe, SrSe and BaSe (Table 7A). In CaO and SrS powders the stability of the  $F_C^+$ -centre was far less than that in MgO, since heating at 300°C was enough to destroy their centres. They accounted this due to a much reduced binding energy of the electron in the  $F_C^+$ -centre in CaO and SrS than in MgO, rather than a stronger tendency for the vacancy pair to dissociate into single vacancies at this temperature.

As mentioned earlier bound vacancy-pairs are energetically favourable in ionic solids as a result of the strong electrostatic attraction between the oppositely charged vacancies. At high temperature the vacancies become mobile and there is an increased probability that the oppositely charged vacancies will combine to produce a neutral divacancy. The decreased concentration of the  $F^+$ -band which accompanies the increased concentration of  $F_C^+$ -centres is presumably due to the thermally activated migration of cation vacancies to  $F^+$ -centres so forming  $F_C^+$ -centres. When the binding energy of the electron to this vacancy pair is small then quite moderate temperatures are capable of ionising this defect, the electron then prefers to reside at deeper lying traps.

In MgO the diffusion of vacancies after neutron irradiation proceeds at lower temperatures than Wertz et al<sup>(1)</sup> originally suggested; even at 250°C  $F_C^+$ -centres are produced in measurable concentrations<sup>(2)</sup>. Above about 600°C thermal ionization effects become apparent, although  $F_C^+$ -centres may be regenerated by X-irradiation. Above 900°C the concentration of  $F_C^+$ -centres which can be regenerated rapidly decreases mainly due to the divacancy migrating to form larger aggregates. Detailed studies have led Henderson and Bowen<sup>(3)</sup> to suggest that the divacancy is the precursor to the formation of voids which are present after high temperature heat treatment. Presumably the vacancy pair must become mobile at even lower temperatures in CaO and SrS.

### 3.2 The g-shift and hyperfine splitting of $F_C^+$ -centres

Wertz et al<sup>(1)</sup> were able to give a qualitative interpretation of the g-shifts reported in Table 5A and of the asymmetry of the  $F_C^+$ -line shape based on the theoretical consideration of Kahn and Kittel<sup>(4)</sup> for F-centres in KCl. Kahn and Kittel showed that as a result of the unsymmetrical electric field associated with the vacancy polarizing the  $K^+$  ions, the normally pure  $|4s\rangle$  state of the valence electron on the neighbouring cation is admixed with some higher lying  $|4p\rangle$  states. A molecular orbital wave function constructed out of the valence states of the six

neighbouring cations will have the form

$$\psi_1 = \psi_s - \frac{\epsilon}{\sqrt{2}} (\psi_p - \psi_p^{-1}) \quad (3.1)$$

where  $\epsilon$  depends upon the energy separation between the  $|4s\rangle$  and  $|4p\rangle$  levels, and the associated electric dipole moment points inwards to the vacancy. Spin orbit interaction of the form  $\lambda$  L.S with the  $|4p\rangle$  states then results in a  $g$  shift given by

$$\Delta g = - \frac{4}{3} \frac{\lambda}{\Delta} \left( \frac{\epsilon^2}{1+\epsilon^2} \right) \quad (3.2)$$

The calculated  $g$ -shift is for the alkali halide F-centres too small compared with experiment but agrees in order of magnitude.

Since the  $F_C^+$ -electron is chiefly concentrated inside the negative ion vacancy, its ground state may be regarded as mainly  $s$ -like and consequently Equation 3.2 should apply. However the lower symmetry of the divacancy relative to the single vacancy, should increase the polarization of the surrounding ions and a larger admixture of the  $|p\rangle$  states is expected. The presence of the positive ion vacancy also displaces the centre of the electron charge cloud towards that cation disposed along the tetragonal axis of the defects (see Fig. 1). This also increases the amount of  $|p\rangle$  character in the ground state wavefunction. Therefore we would expect  $\epsilon$  to increase and the  $g$ -value to be lower than that of the  $F^+$ -centre, as has been confirmed by experiment.

The asymmetry of the line shape depends upon the magnitude of both  $g_{11}$  and  $g_{\perp}$ . The difference between  $g_{11}$  and  $g_{\perp}$  is quite small on account of the small admixture of  $|p\rangle$  character in the ground state wavefunction. For powder samples, all directions of the axis of the defect are equally probable. The probability that the axis of an  $F_C^+$ -centre lies along the direction of the magnetic field is therefore much less than the probability that the axis is perpendicular to the field. If  $g_{11}$  is greater than  $g_{\perp}$ , then the high field portion of the derivative curve (the line shape recorded in an ESR experiment) will be much larger and narrower than the low-field portion. According to Wertz et al the appearance of the  $F_C^+$ -line is in agreement with the above assumptions. It is to be noted that for MgO the measured g-value at Q band<sup>(5)</sup> is such that  $g_{\perp} > g_{11}$ . This cannot be explained by the above simple picture, and the reason for the observation is unknown.

From the structure of the defect as shown in Fig. 1, the presence of the positive ion vacancy will force the electron to move more towards the axially disposed cation at (0,0,-a) and therefore leave this cation and the other four nearest cations inequivalent, i.e. the electron wave function will be more concentrated upon the axial cation than the four cations perpendicular to the axis. This is confirmed essentially by the recently reported measurement of the hyperfine splittings of the  $F_C^+$ -centre in MgO<sup>(5)</sup>. These measurements give an isotropic hyperfine constant of 17.5 gauss for the

axial  $^{25}\text{Mg}^{2+}$  ion while that for the other four ions situated in the (0,1,0) plane is estimated to be less than 2 gauss. Although this is discussed more fully in the next chapter, it is noted that this behaviour is commensurate with the movement of the  $F_C^+$ -electron towards the axial  $\text{Mg}^{2+}$  ion. More evidence is provided by the intensity of the hyperfine lines<sup>(2)</sup>. The expected contribution of hyperfine lines from the single cation is about 10% of the total since this is the probability of the  $F_C^+$ -centres having that particular site occupied by a  $^{25}\text{Mg}$  nucleus, which is the only isotope of Mg that has a nuclear spin of 5/2. There should also be a contribution amounting to 32% of the total intensity arising from those centres in which one or more of the four equivalent cation sites are occupied by  $^{25}\text{Mg}$  nuclei. These expectations are substantially supported by the experimental results at both X and Q bands. When the magnetic field is along a trigonal axis of the crystal, the hyperfine spectrum as shown in Fig 1 consists of a six-line spectrum centred on the main line. This spectrum is some 10-20% of the intensity of the main line. This result clearly suggests that the interaction is with just one Mg site neighbouring the defect. The hyperfine splitting for the single cation is almost four times as large as that of the  $F^+$ -centre, which clearly indicates that the  $F_C^+$ -electron has been drawn closer to the single

cation.

### 3.3 Optical properties of $F_C^+$ -centres

The optical properties of the  $F_C^+$ -centre in alkaline earth oxides have not been studied extensively by experiment, because of the many other optical bands present in annealed crystals. The work of King and Henderson<sup>(6)</sup> on the bleaching efficiency of the centre in MgO indicated a maximum efficiency at about 3.6 eV. In their works they estimated the  $F_C^+$ -centre transition energy by measuring the decay of the  $F_C^+$ -centre as a function of bleaching time using monochromatic radiation of wavelengths in the range 2500-6500Å. For this purpose the amplitude of the  $F_C^+$ -centre resonance line was measured by comparison with that of the  $M_n^{2+}$  lines, since the latter do not change during the experiments. This is to be compared with the calculated results<sup>(5)</sup> of 2.02 eV using a simple continuum model, i.e. an electron trapped by a dipole immersed in a solid dielectric. We shall discuss this calculation in detail in the next chapter. The unpublished results of Stoneham indicates that there is no other bound state exist within 0.01 eV of the bottom of the conduction band. Although these calculations are only approximate, they do point to the fact that the defects should in all cases be bleachable with photons of appropriate energy. The results of King and Henderson substantially support this view in magnesium oxide.

References

1. J.E. Wertz, J.W. Orton and P. Auzins, Disc. Fara. Soc (1961).  
J.E. Wertz, J.W. Orton and P. Auzins, J. Appl. Phys. Supp. (1962).  
J.E. Wertz, J.W. Orton and P. Auzins, Paramagnetic Resonance 1,  
Edited by Low (1963).  
J.E. Wertz, G.S. Saville, L. Hall and P. Auzins, Proc. Brit.  
Ceram. Soc., (1964).
2. B. Henderson, unpublished data.
3. B. Henderson and D.H. Bowen, to be published.
4. A.H. Kahn and C. Kittel, Phys. Rev., 89, 315, (1953).
5. K.C. To, A.H. Stoneham and B. Henderson, Phys. Rev, 181, 1237 (1969)
6. R.D. King and B. Henderson, Proc. Br. Ceram. Soc., 9, 63, (1967).

CHAPTER IV

CONTINUUM MODEL FOR  $F_C^+$ -CENTRE

4.1 Preliminary Comments

This chapter first reviews Pincherle's<sup>(1)</sup> calculations on the D-centre and then calculates the properties of the  $F_C^+$ -centre in alkaline earth oxides. Pincherle's D-centre is equivalent to our  $F_C^+$ -centre since both consist of an electron trapped in the electrostatic field of a cation anion vacancy pair. The earliest treatments used a continuum model for this centre. The detailed atomistic environment of the centre is replaced by the average macroscopic properties of the solid. In this way the problem is simplified considerably. The experimentally measurable macroscopic property of the solid reveals itself in the form of the dielectric constant  $\epsilon$ . We shall find later that for D-centre or  $F_C^+$ -centre, the high frequency dielectric constant  $\epsilon_\infty$  is to be used since the low frequency or static dielectric constant gives no bound states. However the effective-mass approach should be a good approximation for weakly bound states, where the binding energy is appreciably less than the band gap.

Consider an electron moving in the field of a dipole immersed in a solid dielectric of dielectric constant  $\epsilon_\infty$ . The potential energy of the electron is

$$V = \frac{z}{\epsilon_\infty} \left( \frac{2}{r_1} - \frac{2}{r_2} \right) + 2 V_L \quad (4.1)$$

where  $Z$  is the charge of the vacancies forming the dipole, and  $r_1$  and  $r_2$  are the distance of the electron from the positive and negative end of the dipole respectively,  $V_L$  is the potential energy of the electron in the field of the perfect lattice. The Schrödinger Equation may then be written as

$$\left[ -\nabla^2 + \frac{Z}{\epsilon_\infty} \left( \frac{2}{r_1} - \frac{2}{r_2} \right) + 2 V_L \right] f(r) = E_t f(r) \quad (4.2)$$

If we assume that the total wave function is

$$f(r) = \Psi(r) u_0(r) \quad (4.3)$$

where  $u_0(r)$  is the lowest state of the conduction band

$$\left[ -\nabla^2 + 2 V_L \right] u_0(r) = E_0 u_0(r) \quad (4.4)$$

then  $\Psi(r)$  satisfies

$$\left[ -\nabla^2 + \frac{Z}{\epsilon_\infty} \left( \frac{2}{r_1} - \frac{2}{r_2} \right) \right] \Psi(r) = E \Psi(r) \quad (4.5)$$

where  $E = E_t - E_0$  is the energy of the  $F_C^+$ -electron with respect to the bottom of the conduction band  $E_0$ . In the following we consider only Eq. (4.5) assuming the band structure to be known. Because of the axial symmetry of the dipolar field, it is most convenient to work in elliptical coordinates<sup>(2)</sup> (prolate spheroids) whence,

$$\lambda = \frac{r_1 + r_2}{R}, \quad \mu = \frac{r_1 - r_2}{R}, \quad (4.6)$$

$\phi$  = azimuth about the axis of the fixed charges, and  $R$ , the effective separation between the positive and negative charges, is given by

$$R = \frac{\Xi a}{\epsilon_{\infty}} \quad (4.7)$$

where  $a$  is the lattice parameter. If we write the wave function in the form

$$\Psi = L(\lambda) M(\mu) \Phi(\phi) \quad (4.8)$$

then Eq. (4.5) is separable<sup>(3)</sup>: consequently

$$\frac{d^2 \Phi}{d\phi^2} + m^2 \Phi = 0 \quad (4.9)$$

$$\frac{d}{d\mu} \left[ (1-\mu^2) \frac{dM}{d\mu} \right] + \left[ P^2 \mu^2 - 2R\mu - A - \frac{m^2}{1-\mu^2} \right] M = 0 \quad (4.10)$$

$$\frac{d}{d\lambda} \left[ (\lambda^2 - 1) \frac{dL}{d\lambda} \right] + \left[ -P^2 \lambda^2 + A - \frac{m^2}{\lambda^2 - 1} \right] L = 0 \quad (4.11)$$

where  $m$  and  $A$  are separation constants and the parameter  $P$  is related to the electronic energy  $E$  by

$$P^2 = -\frac{R^2}{4} E \quad (4.12)$$

The solution of Eq. (4.9) is easily found to be,

$$\Phi(\phi) = (2\pi)^{-\frac{1}{2}} e^{\pm im\phi} \quad (4.13)$$

and the solution to Eq. (4.10) is given by Baber and Hasse<sup>(4)</sup> as

$$M(\mu) = \ell^{-P\mu} \sum_{\ell=m}^{\infty} f_{\ell} P_{\ell}^m(\mu) \quad (4.14)$$

Here  $P_{\ell}^m(\mu)$  are associated Legendre polynomials and the  $f_{\ell}$  are numerical coefficients satisfying the recurrence relations

$$\begin{aligned} 2(2\ell-1)(\ell+m+1) \left[ P(\ell+1) + R \right] f_{\ell+1} + (2\ell+3)(2\ell-1) \left[ \ell(\ell+1) + A - P^2 \right] f_{\ell} \\ - 2(2\ell+3)(\ell-m)(P\ell-R) f_{\ell-1} = 0 \end{aligned} \quad (4.15)$$

$$f_{m-1} = 0$$

In order that the series (4.15) converges over the interval  $-1 \leq \mu \leq 1$ , the following continued fraction must be satisfied,

$$-\left[ m(m+1) + A - P^2 \right] = \frac{a_{m+1}}{b_{m+1} + \frac{a_{m+2}}{b_{m+2} + \dots}} \quad (4.16)$$

where

$$a_{m+1} = 4 \left[ P^2(m+1)^2 - R_1^2 \right] \quad (4.17)$$

$$a_{\ell} = 4 (\ell^2 - m^2) \left[ P^2 \ell^2 - R_1^2 \right], \quad \ell = m+2, \dots \quad (4.18)$$

$$b_{\ell} = (2\ell+1) \left[ \ell(\ell+1) + A - P^2 \right], \quad \ell = m+1, \dots \quad (4.19)$$

The solution to Eq. (4.11) given by Hylleraas<sup>(5)</sup> is,

$$L(\lambda) = (\lambda^2 - 1)^{\frac{m}{2}} e^{-\frac{x}{2}} \sum_{n=0}^{\infty} \frac{C_n}{(m+n)!} L_{m+n}^m(X) \quad (4.20)$$

where  $X = 2p(\lambda-1)$ , the  $L_{m+n}^m(X)$  are associated Laguerre polynomials<sup>(6)</sup>

and  $C_n$  satisfy

$$(n+m)n C_{n-1} - \left[ 2n^2 + 2n(2p+m+1) - Y \right] C_n + (n+1)(m+n+1) C_{n+1} = 0 \quad (4.21)$$

with

$$Y = A - P^2 - (m+1)(2p+1) \quad (4.22)$$

In order that the series (4.21) converges in the interval  $0 \leq x \leq \infty$ , the following continued fraction must be satisfied

$$-\frac{Y}{m+1} = \frac{a_1}{b_1 - \frac{a_2}{b_2 - \dots}} \quad (4.23)$$

with

$$a_1 = 1 \quad (4.24)$$

$$a_n = \frac{(n+m)n}{(n+m-1)(n-1)}, \quad n = 2, 3, \quad (4.25)$$

$$b_n = \frac{2n^2 + 2n(2p+m+1) - Y}{n(n+m)}, \quad n = 1, 2, \quad (4.26)$$

Eq. (4.16) and (4.23) then determine the eigenvalue of the problem.

#### 4.2 Pincherle's calculations on D-centre

Since we are interested only in the binding energy of the D-centre, we consider only the ground state for which  $m = 0$ .

Eqs. (4.10) and (4.11) then reduce to

$$\frac{d}{d\mu} \left[ (1-\mu^2) \frac{dM}{d\mu} \right] + \left[ P^2 \mu^2 - \beta\mu - A \right] M = 0 \quad (4.27)$$

$$\frac{d}{d\lambda} \left[ (\lambda^2-1) \frac{dL}{d\lambda} \right] + \left[ -P^2 \lambda^2 + A \right] L = 0 \quad (4.28)$$

where we have defined a new parameter  $\beta = 2R$ . Pincherle<sup>(1)</sup> showed that for small values of  $\beta$ ,

$$A = F_1 + F_2 P^2 \quad (4.29)$$

where  $F_1$  and  $F_2$  are numerical constants determined by Eq. (4.16).

Instead of solving the Eqs. (4.16) and (4.23) directly, Pincherle

proceeded to find the solution to Eq. (4.28) by the variational

technique. First he transformed Eq. (4.28) to a form suitable for

the use of variation calculation. He defined

$$L = (\xi^2-1)^{-\frac{1}{2}} \psi_t \quad (4.30)$$

and

$$q(x) = -\frac{F_1}{x(x+2)} - \frac{1}{x^2(x+2)^2}$$

$$W(x) = \frac{(x+1)^2 - F_2}{x(x+2)}$$

where  $x = \xi - 1$ , and  $\xi = \frac{\lambda Z}{\epsilon_\infty}$

Eq. (4.28) then becomes

$$\frac{d^2 \psi_t}{dx^2} - \left[ q(x) + p^2 W(x) \right] \psi_t = 0 \quad (4.31)$$

The variational problem is therefore the minimization of

$$Q = \int_0^\infty \left[ \left( \frac{d\psi_t}{dx} \right)^2 + q(x) \psi_t^2 \right] dx \quad (4.32)$$

subject to the condition 
$$N = \int_0^\infty W(x) \psi_t^2 dx = 1 \quad (4.33)$$

The eigenvalue  $p^2$  playing the role of the Lagrangian multiplier.

Pincherle used as a trial wave function for the ground state

$$\psi_t = c x e^{-\gamma x} \quad (4.34)$$

in which  $C$  is the normalization constant dependent on  $\gamma$ , and  $\gamma$  is the variational parameter. The most interesting result he obtained was that the eigenvalue was determined solely by the parameter  $F_1$  when the variational parameter  $\gamma$  is small. He found that

$$\gamma = .314 F_1 - .179 \quad (4.35)$$

With the result that there will have no bound state for  $F_1 < 0.5$ .

Calculations were carried out for AgBr and PbS only, and from the results shown in Table 5, it is seen that the binding energy is small for PbS. The binding energy for a second electron was found to be effectively zero.

#### 4.3.1 Binding energy of $F_C^+$ -centre in alkaline earth oxides

The binding energy and hyperfine constants for the  $F_C^+$ -centre in the four alkaline earth oxides have been calculated<sup>(7)</sup> using an effective mass approach based on the calculations of Wallis, Herman and Milnes<sup>(3)</sup> for an electron bound in the field of a finite dipole. While the calculations of WHM is for an electron bound in the field of a free dipole, the  $F_C^+$ -centre is immersed in a solid dielectric. Consequently we need to interpolate WHM's calculation for a free dipole to the related system in which the dipole is immersed in a solid dielectric.

The Schrödinger Equation now becomes,

$$\left[ -\nabla^2 + \frac{z}{\epsilon_\infty} \left( \frac{2}{|r-R_+|} - \frac{2}{|r-R_-|} \right) \right] \psi = E\psi \quad (4.36)$$

all energies are referred to the bottom of the conduction band and the high frequency dielectric constant is used. For the four alkaline earth oxides Pincherle's calculations gives  $F_1 < 0.5$  when the static dielectric constants are used in Equation 4.29 and consequently the  $F_C^+$ -centres according to Eq. (4.35) will have no bound states.

Therefore we use the high frequency dielectric constant throughout this calculation. Accordingly it is easily shown<sup>(7)</sup> that

$$\text{Binding Energy} \times (\text{length of dipole})^2 = \text{constant} \quad (4.37)$$

at constant dipole moment. The effective dipole length is then given by

$$R = \frac{Za}{\epsilon_{\infty}} \quad (4.38)$$

The interpolation formula is therefore simply

$$\text{Binding Energy } E_B = (\text{Tabulated } E_B) (R/a)^2 : \quad (4.39)$$

In this equation tabulated  $E_B$  refers to the energies of an electron in the field of a dipole of separation  $R$  calculated by WHM and tabulated in their paper<sup>(3)</sup>. The results of this calculation are shown in Table 6, together with the ratio of the binding energy to the band gap. It is seen that this ratio is rather small and this means that the effective mass approach should be a good approximation. A comparison of the calculated binding energy of the  $F_C^+$ -centre in MgO (2.02 ev) with experiment (3.60 ev)<sup>(8)</sup> shows that the calculated binding energy is too small. This is perhaps not surprising in view of the simplicity of the model. The only excited states lie within about 0.01 ev of the conduction band. Optical absorption should occur at energies higher than this binding energy to states within the conduction band. It is clear that, as the lattice parameter

increases, the transition energy decreases, as for all other colour centres in ionic crystals.

#### 4.3.2 Hyperfine constants of $F_C^+$ -centre in alkaline earth oxides

The isotropic hyperfine constant for the  $F_C^+$ -centre in MgO has been calculated<sup>(7)</sup> using (4.14) and (4.20) and the information given in<sup>(3)</sup>. In this section we shall extend this calculation to CaO, SrO and BaO. As is well known that the isotropic or Fermi contact<sup>(9)</sup> interaction is proportional to the square of the electronic wave function at the nucleus. The hyperfine constant is usually measured in ESR experiments as the separation between two consecutive lines in a hyperfine pattern with the magnetic field as the ordinate. Therefore it is convenient to express the constant in Gaussian units.

$$\frac{A_s}{h} \text{ (Gauss)} = 284.7 \frac{\mu_N}{I_N \mu} \left| \Psi(0) \right|^2 \text{ a.u.}^{-3} \quad (4.40)$$

where  $\mu_N$  is the magnetic moment of the nucleus,  $\mu$  is the nuclear magneton and  $I_N$  is the nuclear spin of the nucleus.  $\Psi(0)$  is the electron wave function in atomic unit evaluated at the site of the nucleus.  $\mu_N$  is usually expressed in units of  $\mu$  and are tabulated together with  $I_N$  in the book by Ramsey<sup>(10)</sup>.

In order to calculate the hyperfine constants  $A_s$ , it is therefore necessary to have a detail knowledge of the electronic wave function at the site of the nucleus. We only need the ground

state wave function ( $m = 0$ ) and this can be found by using Eqs. (4.14) and (4.20) together with the recurrence relations Eqs. (4.15) and (4.21). The recurrence relations determine the ratio of the  $n$ th coefficients to the first coefficient and the first coefficient is then found by the normalization conditions. We shall outline the general procedure for the calculation of the wave function. Eqs. (4.15) and (4.21) are the so-called three terms recurrence relations which require the asymptotic behaviours at large  $n$ <sup>(6)</sup>. It is found to be most convenient to rearrange the recurrence relations in the following forms:

$$\frac{f_{\ell}}{f_{\ell-1}} = \frac{2\ell(p\ell-R)(2\ell+3)}{(2\ell-1)\{(2\ell+3)[\ell(\ell+1)+A-p^2]+2(\ell+1)[p(\ell+1)+R]\} \frac{f_{\ell+1}}{f_{\ell}}} \quad (4.41)$$

$$\frac{C_n}{C_{n-1}} = \frac{n^2}{2n^2 + 2n(2p+1) - Y - (n+1)^2 \frac{C_{n+1}}{C_n}} \quad (4.42)$$

The asymptotic behaviour is then easily found to be

$$\ell \gg 1 \quad \frac{f_{\ell}}{f_{\ell-1}} = \frac{p}{\ell} \quad (4.43)$$

$$n \gg 1 \quad \frac{C_n}{C_{n-1}} = 1 - 2\sqrt{\frac{p}{n}} \quad (4.44)$$

In order to evaluate the coefficients, we need to know  $p$  and  $A$  corresponding to a specified  $R$  and these can be extrapolated from the tables given in <sup>(3)</sup>. The calculations are then fairly straightforward. It is found that the expansion (4.14) and (4.20) converge rapidly and only two or three terms are sufficient to represent the wave function accurately. The total wave function is to be normalised over the whole space and scaled <sup>(7)</sup> according to 4.3.1. It is found that the scalings actually cancelled each other and have no effect on the wave function. The normalisation then gives the following relation between  $f_o$  and  $C_o$  :

$$f_o C_o = \frac{8}{\sqrt{a^3 (M'L'' - M''L')}} \quad (4.45)$$

where

$$M' = \int_{-1}^{+1} M(u)^2 du \quad (4.46)$$

$$M'' = \int_{-1}^{+1} M(u)^2 u^2 du \quad (4.47)$$

$$L' = \int_0^{\infty} L^2(\lambda) d\lambda \quad (4.48)$$

$$L'' = \int_0^{\infty} L^2(\lambda) \lambda^2 d\lambda \quad (4.49)$$

and  $a$  is the lattice parameter. The integrals (4.46) and (4.47) are evaluated by numerical integration. The integrals appearing in (4.48) and (4.49) can be easily calculated by the use of a general formula of integration of products of Laguerre functions as is given in reference<sup>(6)</sup>. For convenience of future references the total electronic wave functions of the  $F_C^+$ -centre in the four alkaline earth oxides are listed in the appendix.

In the effective-mass model  $\Psi$  is an envelope function which modulated the band functions at the conduction band minimum (see Eq. (4.3)). There seems to be no calculations of conduction band functions for alkaline earth oxides, and consequently we adopt another approach which simply orthogonalises  $\Psi$  to the cation ion core functions. This would be strictly correct only if  $\Psi$  were the result of a pseudopotential calculation. Orthogonalising  $\Psi$  has much the same effect as using  $\psi$  to modulate a band function, and in both cases the main effect is the enhancement of the wave function at the cation nuclei. Thus we calculate the hyperfine constants using:

$$|\Psi\rangle = N \left[ |\psi\rangle - \sum_i \langle i|\psi\rangle |i\rangle \right] \quad (4.50)$$

We assume that  $\psi$  varies slowly over the cation cores, so as to simplify

the overlap integrals,

$$\langle i | \Psi \rangle = \Psi \int_0^{\infty} \phi_i d\tau \quad (4.51)$$

This should be adequate because of the relatively weak binding. The  $Mg^{2+}$  and  $Ca^{2+}$  wave functions used were the free ion functions of Clementi<sup>(11)</sup> together with Slater orbitals while for  $Sr^{2+}$  and  $Ba^{2+}$  only the Slater orbitals were used; overlaps of ions of the host lattice with each other were ignored. The results are given in Table 7 for three distinct sites. If the negative ion vacancy is at  $(0,0,0)$  and the positive ion vacancy at  $(0,0,a)$  then the sites considered were those at  $(a,0,0)$ ,  $(a,a,-a)$  and  $(0,0,-a)$  in Fig. 1. The  $(0,0,-a)$  site on the axis of the centre has the largest constant. It is seen that the use of Slater orbitals has considerably underestimated the hyperfine constants. This is understandable because of the vanishing of 2s and higher s state Slater orbitals at the nucleus. The calculation for MgO show a very good agreement with the experiment for the  $^{25}Mg^{2+}$  ion situated along the tetragonal axis but the agreement is not good for the other sites. It is interesting to compare the ratio of the hyperfine constants for the axial  $Mg^{2+}$  at  $(0,0,-a)$  with the  $Mg^{2+}$  situated at  $(a,0,0)$  with experiment.

We have

	(0,0,-a)	(a,0,0)	ratio
Calculation:	18.07	9.108	~2
Expt.	17.5	~2	~8.8

Apparently therefore the continuum model seriously underestimates the ratio of the two hyperfine constants. We shall see in the next chapter that a calculation taking into account the lattice structure will give a much better result.

References

1. L. Pincherle, Proc. Phys. Soc., A64, 648 (1951).
2. H. Margenau and G.M. Murphy, The Mathematics of Physics and Chemistry.
3. R.F. Wallis, R.C. Herman and H.W. Milnes, J. Mol. Spect., 4, 51 (1960).
4. W.T. Baber and H.R. Hasse, Proc. Cambridge Phil. Soc., 31, 564, (1935).
5. E.A. Hylleraas, Z. Physik, 71, 739 (1931).
6. P.M. Morse and H. Feshbach, Methods of Theoretical Physics, Vol. 1
7. K.C. To, A.M. Stoneham and B. Henderson, Phys. Rev. 181, 1237, (1967).
8. R.D. King and B. Henderson, Proc. Br. Ceram. Soc., 9, 63, (1967).
9. See for example C.P. Slichter, Principles of Magnetic Resonances, for a more general discussion see J.S. Griffith, The Theory of Transition Metal Ions.
10. N.F. Ramsey, Nuclear Moments.
11. E. Clementi, I.B.M., J. of R. and D. Dept., 1956, 9, (Suppl) 2.

CHAPTER V

POINT ION LATTICE CALCULATION ON  $F_C^+$ -CENTRES

5.1 Point Ion Lattice Model for the  $F_C^+$ -Centre

As we showed in Chapter 4 continuum model calculations on  $F_C^+$ -centres in the alkaline earth oxides give a reasonable account of the experimental data. We shall therefore pursue this model further, now taking into account the detail lattice structure using first the point ion model of Gourary and Adrian<sup>(1)</sup> including later the various corrections. We consider specifically the corrections due to polarisation, lattice distortion and finite ion size. From the model of the  $F_C^+$ -centre in the alkaline earth oxides<sup>(2)</sup>, it is clear that the trapped electron charge cloud will be concentrated mainly inside the anion vacancy. If in Fig. 2, we replace the ions of valency  $Z$  by point charges<sup>(1)</sup>, the the electrostatic potential energy of the  $F_C^+$ -electron is

$$V_t = V_F + V \quad , \quad (5.1)$$

with

$$V = \frac{Z}{a} \quad , \quad (5.2)$$

where  $V_F$  is the potential energy of the  $F^+$ -centre, and  $V$  is the potential energy due to the cation vacancy. It is convenient to divide the total Hamiltonian  $H$  of the  $F_C^+$ -electron into a part  $\hat{H}_0$  which is

essentially the  $F^+$ -centre Hamiltonian and a part due to the cation vacancy. Then

$$\hat{H} = \hat{H}_O + 2V. \quad (5.3)$$

where the  $F^+$ -centre Hamiltonian is given by

$$\hat{H}_O = -\nabla^2 + 2 \sum_i V_i \text{ (all surrounding + and - ions),} \quad (5.4)$$

in Rydberg's units. We may consider the potential due to the cation vacancy as a small perturbation on the  $F^+$ -centre Hamiltonian  $\hat{H}$ . The perturbation term  $V$  effectively admixes excited states of the  $F^+$ -centre into the ground state. We consider only the admixture of p-like states, all other higher excited states being ignored. The ground state therefore takes the form

$$\psi = C_s |S\rangle + C_p |P\rangle, \quad (5.5)$$

where  $C_s$  and  $C_p$  are constants to be determined by the perturbation together with the normalization of the total wave function. This leads to the secular equation

$$\begin{pmatrix} \langle P | \hat{H}_O + V | P \rangle - E & \langle P | V | S \rangle \\ \langle S | V | P \rangle & \langle S | \hat{H}_O + V | S \rangle - E \end{pmatrix} = 0, \quad (5.6)$$

where we have made use of the fact that

$$\langle P | \hat{H}_O | S \rangle = 0 \quad (5.7)$$

This follows from a group theoretical argument according to which an integral is non-vanishing only when the direct product of any two of the irreducible representations contains the third<sup>(3)</sup>. It is easily seen that this is not so for Eq. (5.7), because in a cubic group the s - like and p - like orbitals transform respectively as the fully symmetrical irreducible representation  $\Gamma_1$  and the irreducible representation  $\Gamma_4$ <sup>(4)</sup>, while the Hamiltonian  $\hat{H}_0$  is invariant under the full cubic group. The eigenvalue E is found to be

$$E = \frac{1}{2} (E_P + E_S) - \sqrt{\frac{1}{4}\Delta^2 + b^2} \quad (5.8)$$

where  $E_P = \langle P | \hat{H}_0 + V | P \rangle$  (5.9)

$$E_S = \langle S | \hat{H}_0 + V | S \rangle \quad (5.10)$$

$$\Delta = E_P - E_S \quad (5.11)$$

$$b = \langle S | V | P \rangle \quad (5.12)$$

The coefficients of expansion are then given by

$$C_S = \left\{ \frac{1}{2} + \frac{1}{2 \left[ 1 + 4 \frac{b^2}{\Delta^2} \right]^{\frac{1}{2}}} \right\}^{\frac{1}{2}} \quad (5.13)$$

$$C_P = \left\{ \frac{1}{2} - \frac{1}{2 \left[ 1 + 4 \frac{b^2}{\Delta^2} \right]^{\frac{1}{2}}} \right\}^{\frac{1}{2}} \quad (5.14)$$

where the ground state wave function is

$$\psi = C_S |S\rangle - C_P |P\rangle$$

We shall use as trial functions

$$|S\rangle = \frac{\sqrt{\alpha^3}}{7\pi} (1 + \alpha r) e^{-\alpha r} \quad (5.15)$$

$$|P\rangle = \frac{\sqrt{\beta^5}}{\pi} r e^{-\beta r} \cos \theta, \quad (5.16)$$

which were also the trial functions we used for our  $F^+$ -centre calculation in Chapter 2.

Our problem is therefore to minimise Eq. (5.8) with respect to the variational parameters  $\alpha$  and  $\beta$ . The relevant energy integrals are derived in the Appendix. We shall adopt Newton-Raphson's method to minimise the total energy, as for the  $F^+$ -centre in Chapter 2. The process is now complicated by the involvement of two variational parameters instead of one. The logical step would be to use the variational parameters  $\alpha$  and  $\beta$  from the  $F^+$ -centre calculation as a first trial parameter for the Newton-Raphson's method. But in fact it became necessary to decrease the  $F^+$ -centre parameters by about .1 for the process to be convergent. The results of the calculations are shown in Table 8. It is seen that the calculated energies decrease with increasing lattice parameter as it should be. Furthermore the admixture of p-like function into the ground state is about 19% for all the four alkaline earth oxides, there being a slight increase with the increase of lattice parameter. As we shall see in the next section,

the admixture will be reduced if the centre of the charge cloud is allowed to move towards the cation disposed along the tetragonal axis. The point ion lattice model clearly over estimates the binding energy, especially for the heavier oxides with their high polarisability and large ion sizes.

## 5.2 Polarisation and Lattice Distortion Corrections

In a perfect cubic crystal the electrostatic fields at a lattice site balance each other and the polarisation effects are negligible. The existence of an anion vacancy will give rise to an effective electrostatic field proportional to the valency of the absent anion. This electric field will polarise the surrounding ions and this polarisation then reacts back on the trapped electron (see Chapter 2). A cation vacancy will similarly polarise the surrounding ions but because of the charge difference of a cation vacancy the induced dipoles will have a different direction from that due to the anion vacancy. The combination of an anion-cation vacancy pair will therefore have very different polarisation effects from those of the single anion vacancy. First we consider only the polarisations of the nearest cations and the nearest anions neighbouring the anion vacancy and also the nearest anions to the cation vacancy. The relevant ions are shown in Fig. 2. We allow only the nearest cations and anions to the vacancy pair to move, their new position being given

by  $(1 + \sigma)a$ . The anions labeled A and B in Fig. 2 are held stationary at their normal sites. Furthermore the centre of the charge cloud associated with the trapped electron is allowed to move a distance  $\gamma a$  towards the cation disposed at the tetragonal axis. The sign conventions are best illustrated by expressing the "distance" of the  $i$ th site from the centre of the trapped electron in the following form:

$$R_i = \{x_i^2 + (y_i + \sigma_2 a)^2 + (z_i + \sigma_4 a - \sigma_1 a + \gamma a)^2\}^{\frac{1}{2}} \quad (5.17)$$

$$|\sigma_2| = |\sigma_4| = |\sigma_1| = |\sigma| \quad ,$$

where  $x_i$ ,  $y_i$  and  $z_i$  are the cartesian coordinates of the  $i$ th site with respect to the centre of the anion vacancy, and  $\sigma_2$  is the displacement of the ions disposed at positions perpendicular to the axis of the vacancy pair,  $\sigma_1$  is the displacement of the cation disposed along the tetragonal axis of the vacancy pair and  $\sigma_4$  is the displacement of the anion also disposed at the axis of the vacancy pair. In the use of Eq. (5.17) we shall put  $\sigma_2 = \sigma_4 = 0$  if we are considering  $\sigma_1$  and  $\sigma_1 = \sigma_4 = 0$  if we are considering  $\sigma_2$  and similarly for  $\sigma_4$ .

We further assume that the induced dipole moments can be separated into rectangular components  $(p_{ix}, p_{iy}, p_{iz})$ . The following is a list of typical dipole moments of the various sites under consideration:

$$(0, a, 0) \text{ site} : (0, P_{2y}, P_{2z}) \quad (5.18)$$

$$(0, 0, -a) : (0, 0, P_{1z}) \quad (5.19)$$

$$(0, a, a) : (0, P_{3y}, P_{3z}) \quad (5.20)$$

$$(0, 0, 2a) : (0, 0, P_{4z}) \quad (5.21)$$

$$(0, a, -a) : (0, P_{Ay}, P_{Az}) \quad (5.22)$$

$$(a, a, 0) : (P_{By}, P_{By}, P_{Bz}) \quad (5.23)$$

The other sites not listed can be obtained from Equations 5.18 to 5.23: e.g. the dipole moment for  $(-a, 0, 0)$  is found by rotating Eq. (5.18) and is  $(-P_{2y}, 0, P_{2z})$ .

#### 5.2.1. Depolarisation Factors

As for the  $F^+$ -centre, it is convenient to divide the "depolarisation factors" into two groups, one due to ions such as the four  $(0, a, 0)$  ions disposed around the axis and the other due to the interactions among the other highly symmetrical groupings above. In calculating the depolarisation factors lattice distortions are ignored for simplicity. The electrostatic field due to a dipole of moment  $p$  is

$$E = -\frac{\vec{P}}{R^3} + \frac{3\vec{P} \cdot \vec{R}}{R^5} \vec{R} \quad (5.24)$$

Applying Eq. (5.24) to the four  $(0, a, 0)$  ions shows that the Y-component of the electrostatic field at a particular site due to the other 3 sites is given by

$$E_{2y}'' = -\frac{1}{a^3} \left( \frac{1}{4} + \frac{3\sqrt{2}}{4} \right) P_{2y} \quad (5.25)$$

and that the Z component is given by

$$E_{2z}'' = -\frac{1}{a^3} \left( \frac{1}{8} + \frac{1}{\sqrt{2}} \right) P_{2z} \quad (5.26)$$

The induced dipole moment is given by

$$P_{2y} = \alpha^+ (E_{2y}' + E_{2y}'') \quad (5.27)$$

$$P_{2z} = \alpha^+ (E_{2z}' + E_{2z}'') \quad (5.28)$$

where  $\alpha^+$  is the polarisability of the cations and  $E_{2y}'$  and  $E_{2z}'$  denote the electric field at the site other than the field from the other 3 ions. The combination of Eqs. (5.25) and (5.27) and Eqs. (5.26), (5.28) then gives

$$P_{2y} = K_{2y} \alpha^+ E_{2y}' \quad (5.29)$$

$$P_{2z} = K_{2z} \alpha^+ E_{2z}' \quad (5.30)$$

where

$$K_{2y} = a^3 / \left[ a^3 + \alpha^+ \left( \frac{1}{4} + \frac{3\sqrt{2}}{4} \right) \right] \quad (5.31)$$

$$K_{2z} = a^3 / \left[ a^3 + \alpha^+ \left( \frac{1}{\sqrt{2}} + \frac{1}{8} \right) \right] \quad (5.32)$$

are the depolarisation factors for the four sites. Similarly the depolarisation factors for the four (0, a, a) sites are,

$$K_{3y} = a^3 / \left[ a^3 + \alpha^- \left( \frac{1}{4} + \frac{3\sqrt{2}}{4} \right) \right] \quad (5.33)$$

$$K_{3z} = a^3 / \left[ a^3 + \alpha^- \left( \frac{1}{8} + \frac{1}{\sqrt{2}} \right) \right] \quad (5.34)$$

and that for the four (0, a, -a) sites,

$$K_{Ay} = K_{3y} \quad (5.35)$$

$$K_{Az} = K_{3z} \quad (5.36)$$

and for the four (a, a, 0) sites

$$K_{By} = a^3 / \left[ a^3 + \left( \frac{3}{8} + \frac{1}{8\sqrt{2}} \right) \alpha^- \right] \quad (5.37)$$

$$K_{Bz} = a^3 / \left[ a^3 + \alpha^- \left( \frac{1}{4} + \frac{1}{16\sqrt{2}} \right) \right] \quad (5.38)$$

The second part of the depolarisation factor consists of interactions among the various groupings of ions such as the four (0, a, 0). In general the  $j$ th component of the induced dipole moment at the  $i$ th site can be represented as

$$P_i^j = \sum_{q=1}^2 \sum_{k=1}^6 D_{ikq}^j E_{kq} \quad (5.39)$$

where  $E_{kq}$  are the  $q$ th component of the electrostatic field other than the dipolar field at the  $k$ th site, i.e.  $E_{kq}$  consists of the  $q$ th component such as the  $Y$ -component of the electrostatic field due to the vacancies, the trapped electron and the displacements of the ions at the  $k$ th site.  $D_{ikq}^j$  are the depolarisation factors which depend on the geometrical arrangements of ions and their polarisabilities. The calculation of  $D_{ikq}^j$  is rather tedious and only the general procedure is outlined. First we notice that the induced dipole moment is proportional to the total electric field at the site under consideration (see Eqs. (5.27) and (5.28)). The total electric field is in turn partially due to the induced dipole moments at other sites. Therefore we can write down the following expressions

$$P_i^j = \alpha^i K_{ij} E_{ij} + \sum_{n,q \neq i,j} a_{q,n} P_n^q, \quad (5.40)$$

where  $\alpha^i$  is the polarisability of the  $i$ th ion and  $k_{ij}$  are the first depolarisation factor given in Eqs. (5.31) to (5.38),  $a_{qn}$  are constants dependent on the geometrical arrangements of the dipoles. We may rearrange Eq. (5.40) in the following form

$$P_i^j - \sum_{n,q \neq i,j} a_{q,n} P_n^q = \alpha^i K_{ij} E_{ij} \quad (5.41)$$

There are ten equations of the form (5.41), because the electric field at the two axially disposed ions have  $Z$ -components only. Therefore to find  $P_i^j$  or  $D_{ikq}^j$  we have to solve 10 simultaneous linear equations.

It is perhaps simplest to solve the equations by successive elimination. Consider for example the pair of ions (0,a,0) and (a,a,0). We shall use the subscript 2 to represent the first ion and subscript B to represent the second, then

$$P_{2y} = \alpha^+ K_{2y} (E'_{2y} - \frac{2.465}{a^3} P_{By}) \quad (5.42)$$

$$P_{By} = \alpha^- K_{By} (E'_{By} - \frac{1.233}{a^3} P_{2y}) \quad (5.43)$$

where  $E'_{2y}$  stands for the total field at (0,a,0) minus the dipolar field due to the ion at (a,a,0), and similarly for  $E'_{By}$ . The solution to Eqs. (5.42) and (5.43) may therefore be written as

$$P_{2y} = F_{22} E'_{2y} - F_{2B} E'_{2B} \quad (5.44)$$

$$P_{By} = F_{B2} E'_{2y} + F_{BB} E'_{By} \quad (5.45)$$

where

$$F_{22} = \alpha^+ K_{2y} / \left[ 1 - 3.2 \alpha^- \alpha^+ K_{By} K_{2y} / a^6 \right] \quad (5.46)$$

$$F_{2B} = \frac{(2.465 \alpha^- \alpha^+ K_{By} K_{2y})}{a^3} / \left[ 1 - 3.2 \alpha^- \alpha^+ K_{By} K_{2y} / a^6 \right] \quad (5.47)$$

$$F_{B2} = \frac{1.233 \alpha^- K_{By}}{a^3} F_{22} \quad (5.48)$$

$$F_{BB} = \alpha \bar{K}_{By} + \frac{1.233 \alpha \bar{K}_{By} F_{2B}}{a^3} \quad (5.49)$$

to proceed further we shall split  $E_{2y}$  and  $E_{By}$  into terms that contain the contribution from another dipole moment such as  $P_{Ay}$  and add another equation representing  $P_{Ay}$  to the same order as  $P_{2y}$  and  $P_{By}$ . This process continues till all the dipole moments are expressed in the form of Eq. (5.39). We shall have in all  $10 \times 10 = 100$  different  $D_{ikq}^j$ . The final expressions are too long to write out in detail, but with the use of modern digital computers, the depolarisation factors can be easily evaluated for each particular case. We shall only give the overall depolarisation factors for MgO. We define the overall depolarisation factor as the ratio of the dipole moment when the various dipolar interaction are included to the dipolar moment in the absence of any dipolar interactions, i.e.

$$\bar{D}_i^j = \frac{P_i^j}{\alpha^i E_{ij}} \quad (5.50)$$

we have then for MgO

ion sites (i)	$\bar{D}_i^y$	$\bar{D}_i^z$
(0,a,0)	2.2	.77
(0,0,-a)		.1
(0,a,a)	.76	.8
(0,a,-a)	.79	.92
(a,a,0)	-2.6	.91
(0,0,2a)		.72

### 5.2.2. Electrostatic Field and Energy Changes of the Electron

For simplicity we shall assume that the electrostatic field of the trapped electron at each lattice site depends on  $\gamma$  only while the dependence on  $\sigma$  is ignored, because it is expected that  $\gamma \gg \sigma$ . We also assume throughout these calculations that the variational parameters  $\alpha$  and  $\beta$  remain unchanged. This is because the binding energy is insensitive to small changes in  $\alpha$  and  $\beta$ . Therefore the  $j$ th component of the electrostatic field at the  $i$ th site due to the trapped electron can be expressed as

$$E_{ij}^e (R_i, \gamma) = E_{ijo}^e (R_i) + E_{ij1}^e (R_i) \gamma + \frac{1}{2} E_{ij2}^e (R_i) \gamma^2 \quad (5.51)$$

where  $E_{ijk}^e (R_i)$ ,  $k = 0, 1, 2$  are to be evaluated at each lattice site. Therefore the total electrostatic field at each lattice site is the sum of  $E_{ij}^e (R_i, \gamma)$ , the field due to the vacancies and the change of the electrostatic field due to the lattice displacements. The total fields are then given by

$$E_{kq} = E_{kq}^V + E_{kq}^e + E_{kq}^L \quad (5.52)$$

where  $E_{kq}^V$  and  $E_{kq}^L$  are the  $q$ th components of the electrostatic field at the  $k$ th site due to the vacancy pair and the lattice displacements respectively. These are evaluated in the appendix.

Let us now calculate the electrostatic field due to the trapped electron,  $E_{ij}^e$ . First consider the electrostatic potential due to the electron which takes the form

$$V(R) = q \int_0^{\infty} \frac{\psi^2(r) d\tau}{|r-R|} \quad (5.53)$$

$\psi(r)$  being the electronic wave function given by Eq. (5.5).

Therefore

$$V(R) = q \{ C_s^2 V_s(R) + C_p^2 V_p(R) - 2 C_s C_p V_{sp}(R) \} \quad (5.54)$$

where

$$V_s(R) = \int_0^{\infty} \frac{\psi_s^2(r) d\tau}{|r-R|} \quad (5.55)$$

$$V_p(R) = \int_0^{\infty} \frac{\psi_p^2(r) d\tau}{|r-R|} \quad (5.56)$$

$$V_{sp}(R) = \int_0^{\infty} \frac{\psi_s \psi_p d\tau}{|r-R|} \quad (5.57)$$

Therefore  $E_{ij}^e$ ,  $j = y, z$  are given by

$$E_{iy}^e = -q \left\{ C_s^2 \frac{\partial V_s}{\partial R_i} + C_p^2 \frac{\partial V_p}{\partial R_i} - 2 C_s C_p \frac{\partial V_{sp}}{\partial R_i} \right\} \frac{y_i}{R_i} \quad (5.58)$$

$$E_{iz}^e = -q \left\{ C_s^2 \frac{\partial V_s}{\partial R_i} + C_p^2 \frac{\partial V_p}{\partial R_i} - 2C_s C_p \frac{\partial V_{sp}}{\partial R_i} \right\} \frac{z_i + \gamma}{R_i}$$

$$-q \left\{ C_p^2 \frac{\partial V_p}{\partial z_i} - 2C_s C_p \frac{\partial V_{sp}}{\partial z_i} \right\} \quad (5.59)$$

Our problem is to expand  $E_{iy}^e$  and  $E_{iz}^e$  to second order in  $\gamma$  at the centre of the anion vacancy remembering that  $C_s$  and  $C_p$  also depend on  $\gamma$ . These expansions are given in the appendix.

The lattice distortion correction to the binding energy may be similarly calculated. The binding energy is given by Eq. (5.8).

$$E = \frac{1}{2} (E_p + E_s) - \sqrt{\frac{1}{4} \Delta^2 + b^2} \quad (5.8)$$

The expansion of  $E_p$ ,  $E_s$  and  $b$  in terms of  $\gamma$  are given in the appendix, the expansions in terms of  $\sigma$  may also be similarly found provided that care is taken to use the correct sign convention of Eq. (5.17).

We define

$$Q_0 = \frac{1}{4} \Delta^2 + b^2$$

$$Q_1 = \frac{1}{2} \Delta \frac{\partial \Delta}{\partial \gamma} + 2b \frac{\partial b}{\partial \gamma}$$

$$Q_2 = \frac{1}{2} \Delta \frac{\partial \Delta}{\partial \sigma} + 2b \frac{\partial b}{\partial \sigma}$$

$$Q_3 = \frac{1}{4} \left\{ \left( \frac{\partial \Delta}{\partial \gamma} \right)^2 + \Delta \frac{\partial^2 \Delta}{\partial \gamma^2} \right\} + \left\{ \left( \frac{\partial b}{\partial \gamma} \right)^2 + b \frac{\partial^2 b}{\partial \gamma^2} \right\}$$

$$Q_4 = \frac{1}{4} \left\{ \left( \frac{\partial \Delta}{\partial \sigma} \right)^2 + \Delta \frac{\partial^2 \Delta}{\partial \sigma^2} \right\} + \left\{ \left( \frac{\partial b}{\partial \sigma} \right)^2 + b \frac{\partial^2 b}{\partial \sigma^2} \right\}$$

$$Q_5 = \frac{1}{2} \left( \frac{\partial \Delta}{\partial \gamma} \frac{\partial \Delta}{\partial \sigma} + \Delta \frac{\partial^2 \Delta}{\partial \gamma \partial \sigma} \right) + 2 \left( \frac{\partial b}{\partial \gamma} \frac{\partial b}{\partial \sigma} + b \frac{\partial^2 b}{\partial \gamma \partial \sigma} \right)$$

Then the lattice distortion correction to the energy is

$$\begin{aligned} \Delta E_L = & \left\{ .5 \left( \frac{\partial E_D}{\partial \gamma} + \frac{\partial E_S}{\partial \gamma} \right) - .5 \frac{Q_1}{\sqrt{Q_0}} \right\} \gamma \\ & + \left\{ .5 \left( \frac{\partial E_D}{\partial \sigma} + \frac{\partial E_S}{\partial \sigma} \right) - .5 \frac{Q_2}{\sqrt{Q_0}} \right\} \sigma \\ & + \left\{ .25 \left( \frac{\partial^2 E_D}{\partial \gamma^2} + \frac{\partial^2 E_S}{\partial \gamma^2} \right) - (.5 Q_3 - .125 * \frac{Q_1^2}{Q_0}) / \sqrt{Q_0} \right\} \gamma^2 \\ & + \left\{ .25 \left( \frac{\partial^2 E_D}{\partial \sigma^2} + \frac{\partial^2 E_S}{\partial \sigma^2} \right) - (.5 Q_4 - .125 * \frac{Q_2^2}{Q_0}) / \sqrt{Q_0} \right\} \sigma^2 \\ & + \left\{ .5 \left( \frac{\partial^2 E_D}{\partial \gamma \partial \sigma} + \frac{\partial^2 E_S}{\partial \gamma \partial \sigma} \right) - (.5 Q_5 - .25 * \frac{Q_1 * Q_2}{Q_0}) / \sqrt{Q_0} \right\} \sigma \gamma \end{aligned}$$

### 5.2.3. The Lattice Energies

The total change of energy of the system consists of an electronic part which has been considered, and a part due to the lattice. The lattice part of the energy consists of the polarisation lattice interaction and the change of energy due to the vacancies. As we have seen in the case of  $F^+$ -centre that the polarisation lattice interaction consists of two parts. The one which is due to the work done by the ions in the field of the point dipoles is

$$\Delta W_{LC} = 2a \sum_i N_i q_i \int_0^\sigma \vec{E}_i(\sigma_i) \cdot d\vec{\sigma}_i \quad (5.61)$$

where  $E_i(\sigma_i)$  is the dipolar field at the  $i$ th site,  $N_i$  is the number of ions occupying sites equivalent to the  $i$ th site, and  $q_i$  is the charge of the ion at the  $i$ th site. The other which is the work done by the point dipole against all the fields acting on the dipole is

$$\Delta W_{LP} = \sum_i N_i \frac{1}{\alpha_i} \int_0^\sigma \frac{\partial}{\partial \sigma_i} (P_i^2(\sigma_i)) d\sigma_i \quad (5.62)$$

where  $P_i(\sigma_i)$  is the dipole moment at the  $i$ th site which possess a polarisability  $\alpha_i$ .  $\Delta W_{LC}$  and  $\Delta W_{LP}$  are dependent on  $\gamma$  through the dipole moments. The change of the electrostatic energies of the lattice may be shown to be

$$\Delta W_{ee} = \frac{2}{a} \{ -26.693 \sigma + 46.195 \sigma^2 \} \quad (5.63)$$

For the overlap-repulsive term we use  $br^{-\lambda}$ . Then we get

$$\Delta W_{er} = \frac{2 \times 1.165}{a} \left\{ (10 + 2^{2-\lambda/2}) \sigma + \left[ -11 + 5\lambda + (13\lambda-2)2^{-\lambda/2} \right] \sigma^2 \right\} \quad (5.64)$$

The total change of energies of the system is then the sum of (5.60), (5.61), (5.62), (5.63) and (5.64). This sum is to be minimised with respect to  $\sigma$  and  $\gamma$ . The equilibrium values  $\sigma_0$  and  $\gamma_0$  so obtained are then used to calculate the polarisation and lattice distortion correction to the electronic energy. The lattice distortion correction to the energy is given by Eq. (5.60). We shall consider the polarisation correction to the energy. The potential energy of an electron in the field of a dipole is given by

$$V_e = - \vec{P} \cdot \vec{E} \quad (5.65)$$

where  $E$  is given by Esq. (5.58) and (5.59).

The results of the calculation are shown in Table 9, while the dipole moments and the electric field due to the trapped electron are shown in Table 10. It is interesting to see that the polarisation of the surrounding ions act in such a way as to increase the binding energy. A reference to Table 10 shows that this is because of the large dipole moment induced on the anions at  $(0,a,a)$  which are the nearest anions to the cation vacancy. A reference to Fig. 2 shows

that for these anions the electrostatic field of the cation vacancy acts in the same direction as the trapped electron while the total electric field at the 4 nearest cations and the 4 nearest anions to the anion vacancy nearly cancel each other. The net effect of this is therefore an increase of the binding energy due to the polarisation. We should also notice the rapid decrease of the polarisation correction to the energy of the series from MgO to BaO, due to the increase of polarisability of the cations along the series. This is clearly shown in Table 10.

This calculation is not complete because (1) we have not included the ion size and exchange effects, (2) the assumption of a uniform lattice distortion of  $\sigma$  is not justified because the axial ions  $(0,0,-a)$  and  $(0,0,2a)$  may have a different distortion from the other ions even a change of sign cannot be ruled out, (3) the assumption that the polarisability is a scalar that can be taken from the bulk crystals, and (4) the neglect of the polarisable ions other than the nearest neighbour ions. The effects from (2) to (4) are expected to be much less than the ion size effects. Therefore we shall consider in the next section the ion size corrections to the binding energy.

### 5.3 Ion Size Correction

We shall estimate the ion size correction to the binding energy by the method of Bartram, Stoneham and Gash<sup>(5)</sup>. As we have already seen in Chapter 2 in connection with the  $F^+$ -centre in the alkaline earth oxides that this method gives a reasonable account for

the binding energy of the  $F^+$ -centre. We shall apply the same method to the  $F_C^+$ -centre. It is reasonable to suggest that the effect of including finite ion sizes is to slightly increase the distortion and polarisation, because both ion size and exchange concentrate more of the electronic charge inside the vacancies. At the same time an increase of distortion and the ion size will force the electron to move more towards the axial cation, i.e. to increase  $\gamma$ . The net effect of all these together may probably be very small. Therefore we shall assume that the lattice distortion and polarisations are unaffected by the ion size correction, so far as the binding energy is concerned. In the following procedure the ion size correction is applied separately to  $E_s$ ,  $E_p$  and  $b$  as defined in Eqs. (5.9), (5.10) and (5.12). The procedures are then similar to those in Chapter 2, except that we have to consider  $E_s$  and  $E_p$  simultaneously and minimise with respect to two variational parameters. The results are shown in Table 11. Since there is no theoretical calculation of the conduction band minimum for the alkaline earth oxides, the value quoted for MgO (-1.0 eV) is the estimate of Yamashita<sup>(6)</sup>. With this estimation for the conduction band minimum, the binding energy of the  $F_C^+$ -electron in MgO is -4 eV which compares favourably with the experimental value of -3.6 eV<sup>(7)</sup>. For the alkaline earth oxides series from MgO to BaO, the ion size correction accounts for the following percentage of the point ion binding energy: MgO (23.9%),

CaO (26.8%), SrO (25.3%) and BaO (26.8%). It is seen that the ion size effects play a significant role in these oxides. We should like to point out that the success of the ion size correction to the binding energy of the  $F_C^+$ -centre in the alkaline earth oxides is probably due to the small admixture of the excited state which is less than 10% for the four oxides considered.

#### 5.4 The Hyperfine Constants

The isotropic hyperfine constant can be calculated similar to the method used in Chapter 4. According to Equation 4.40 the hyperfine constant is related to the wave function  $\phi(0)$  evaluated at the nucleus concerned by

$$\frac{A_s}{h} \text{ (Gauss)} = 284.7 \frac{\mu_N}{I_N \mu} \left| \phi(0) \right|^2 \text{ a.u.}^{-3} \quad (4.40)$$

The problem is to calculate a suitable wave function at the nucleus. This is usually done in the point ion model by the Schmidt process i.e.,

$$\phi = N \left[ \psi - \sum_i \langle \psi | i \rangle | i \rangle \right] \quad (5.67)$$

where  $N$  is a normalisation constant,  $|i\rangle$  are the ion core orbitals. For the calculation of isotropic hyperfine constants only the  $s$  orbitals of the ion core needed to be considered, since all other orbitals vanish at the nucleus. In this chapter we have considered three different

wave functions  $\Psi$ , i.e. (1) the point ion lattice wave function, (2) the point ion lattice wave function with lattice distortion and polarisation correction and finally (3) the wave function (1) with ion size effects, included. We have assumed in the calculation of lattice distortion and polarisation effects that the variational parameters  $\alpha$  and  $\beta$  remain unchanged. It is argued there that this assumption may have little effect on the binding energy of the electron because of the insensitivity of the binding energy due to small changes in  $\alpha$  and  $\beta$ . This is certainly not quite true for the wave function itself. Therefore the calculations from (2) and (3) must be considered as only qualitatively true under the approximation of the model. The hyperfine constants are calculated by substituting Eq. (5.67) into Eq. (4.40). The core orbitals used in these calculations are the same orbitals as in Chapter 4. The results of the calculation are shown in Table 12. It is interesting to compare for MgO the three cases with that of the continuum model of Chapter 4,

	(0,a,0)	(0,0,-a)	ratio
Continuum Model	9.108	18.07	1.98
point ion	11.052	42.623	3.86
+lattice + polarisation	8.046	54.293	6.76
+ ion size	6.981	42.748	6.14
experimental	~2.00	17.50	~8.80

The results are interesting because they show the obvious improvement of the ratio of the hyperfine constants,  $A_{00-a}/A_{0a0}$ , after the lattice distortion and polarisation correction over the continuum model. This calculated ratio will be further improved if we had allowed the axial ion  $(0,0,-a)$  to distort a different amount than the four  $(0,a,0)$  ions, because it is expected that the former distortion will in general be smaller than the latter distortion because of the attraction of the cation vacancy. The improvement of  $A_S$  after ion size correction is also to be noted. It seems plausible from this calculation that a more sophisticated treatment of the lattice distortion and polarisation plus ion size effects will be able to explain the experimental results at least for MgO.

### 5.5 Conclusions

We shall summarise the assumptions we have made in our calculations: (1) we have assumed in the calculation of lattice distortion that all the movable ions distort the same amount  $\sigma$ . First consider the  $(0,0,-a)$  and  $(0,a,0)$  ions. The cation vacancy at  $(0,0,a)$  can be seen to have a stronger attraction to the former than the latter ion, in the direction shown in Fig. 2. The trapped electron which is constrained to move along the axis of the divacancy in our model will also tend to attract the  $(0,0,-a)$  ion more strongly than the other ions. The combined effects of this will therefore result in a

different distortion at  $(0,0,-a)$  from  $(0,a,0)$ . This will in general increase the binding energy. Consider then the ions at  $(0,a,0)$  and  $(0,a,a)$ . Without the trapped electron these two ions should have the same distortion in the Y direction and even move a little towards each other in the Z direction. The trapped electron will pull the cations at  $(0,a,0)$  towards the centre of the anion vacancy and push the anions at  $(0,a,a)$  outwards from the cation vacancy. Therefore it is expected that the distortion at  $(0,a,0)$  will be less than that at  $(0,a,a)$ . As we have seen in section 5.3 that the anions at  $(0,a,a)$  are chiefly responsible for the polarisation correction; an increase of distortion at  $(0,a,a)$  will therefore reduce the polarisation correction to the energy. We believe that a relaxation of the condition of uniform distortion will in general lead to a larger distortion and therefore increase the lattice distortion correction to the energy. A complete study of the lattice distortion including the shift of the charge centre of the trapped electron along these lines is hindered by the lack of suitable methods of taking the ion size effects into account. We believe that the combined effects of all these is to reduce the binding energy. (2) In our use of the ion size correction of Bartram, Stoneham and Gash, we have assumed that the lattice distortion and polarization correction to the binding energy is unaffected by the ion size correction. (3) We have also assumed that the electrostatic field at the lattice sites due to the trapped electron is so smooth

that the change due to lattice distortion may be neglected, see Eq. (5.51) If this variation was taken into account, the polarisation correction would be reduced and we would expect a decrease of the binding energy.

(4) The variation parameters  $\alpha$  and  $\beta$  have been treated as constants for the lattice distortion and polarisation correction. From a physical point of view, the parameters are related to the kinetic energy of the trapped electron. If the trapped electron has been drawn closer to the axial ion at  $(0,0,-a)$  we would expect an increase of  $\alpha$  and  $\beta$  because now the volume of the electron motion is reduced, from the uncertainty principle. We would therefore expect a decrease of the binding energy due to the increase of kinetic energy. It is assumed throughout our calculation that this change of energy is quite negligible as compared with other corrections to the energy. But we are not quite justified in making this assumption in the calculation of hyperfine constants.

Because of the lack of experimental data for the alkaline earth oxides, other than MgO we are unable to compare our calculations with the experiment, in detail. For MgO where experimental results are available, our calculation compares favourably with the experiment. For the other oxides we believe that our results represent an upper bound for the binding energy. Although the absolute value of the hyperfine constant from this point ion model calculation is too large compared with experiment, the improvement of the ratio of the hyperfine constant in this model is quite encouraging. The results of our calculation from both the continuum model and the point ion model demonstrate that the model of the  $F_C^+$ -centre as consisting of an electron trapped in an anion-cation vacancy pair is quite realistic and justified.

References

1. B.S. Gourary and F.J. Adrian, Phys. Rev. 105, 1180, (1957).
2. J.E. Wertz, J.W. Orton, P. Auzins, Discuss. Faraday Soc., 30  
40, (1961).
3. M. Hamermesh, Group Theory and its application to Physical  
Problems, (1962).
4. H.A. Bethe, Splitting of Terms in Crystals, Consultants Bureau, N.Y.
5. R.H. Bartram, A.M. Stoneham and P. Gash, U.K.A.E.A. Pub. No. HL68/35
6. J. Yamashita, Phys. Rev. 111, 733, (1958).
7. R.D. King and B. Henderson, Proc. Br. Ceram. Soc., 9, 63, (1967).

APPENDIX

(A) Nuclear Attraction Integrals

If we assume that the wave functions have the following form:

$$|s\rangle = a(r) \tag{1}$$

$$|p\rangle = b(r) r \cos\theta \tag{2}$$

then the various nuclear attraction integrals will be, in units of  $\frac{Ze^2}{R}$ ,

$$\langle s | \frac{Ze^2}{|r-R|} | s \rangle = 1 + \frac{\int_R^\infty dr a^2(r) [r R - r^2]}{\int_0^\infty dr a^2(r) r^2} \tag{3}$$

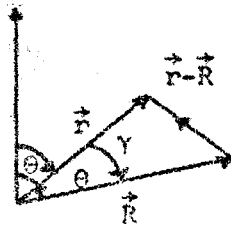
$$\langle p | \frac{Ze^2}{|r-R|} | p \rangle = 1 + \frac{\int_R^\infty dr b^2 [r^3 R - r^4]}{\int_0^\infty dr r^4 b^2}$$

$$+ \frac{2}{5} \frac{(3n^3 - 1)}{2} \frac{\frac{1}{R^2} \int_0^R dr r^6 b^2 + R^3 \int_R^\infty dr r b^2}{\int_0^\infty dr r^4 b^2} \tag{4}$$

$$\langle p | \frac{ze^2}{|r-R|} | s \rangle = \frac{n}{\sqrt{3R}} \frac{\int_0^R dr r^4 ab + R^3 \int_R^\infty dr r ab}{\sqrt{\int_0^\infty dr r^2 a^2 \int_0^\infty dr r^4 b^2}} \quad (5)$$

where  $n = \cos \theta$  is the cosine of the angle which the vector  $\vec{R}$  forms with the polar axis.

We shall only consider the derivation of (5), the other integral may be similarly derived



With reference to the above sketch, we have

$$\begin{aligned} r < R, \quad \frac{1}{|r-R|} &= \sum_{\ell=0}^{\infty} \frac{r^\ell}{R^{\ell+1}} P_\ell (\cos \gamma) \\ &= \sum_{\ell=0}^{\infty} \frac{4\pi}{2\ell+1} \frac{r^\ell}{R^{\ell+1}} \sum_{m=-\ell}^{+\ell} Y_{\ell m} (\theta, \phi) Y_{\ell m}^* (\theta, \phi) \end{aligned} \quad (6)$$

$$r > R, \quad \frac{1}{|r-R|} = \sum_{\ell=0}^{\infty} \frac{4\pi}{2\ell+1} \frac{R^\ell}{r^{\ell+1}} \sum_{m=-\ell}^{+\ell} Y_{\ell m} (\theta, \phi) Y_{\ell m}^* (\theta, \phi) \quad (7)$$

From the properties of integrals of products of spherical Harmonics, we see that only  $\ell = 1$  would contribute to the integral of Eq. (5), so

$$r < R \quad \frac{1}{|r-R|} = \frac{4\pi}{3} \frac{r}{R^2} \sum_{m=-1}^{+1} Y_{1m}(\theta, \phi) Y_{1m}^*(\theta, \phi) \quad (8)$$

$$r > R \quad \frac{1}{|r-R|} = \frac{4\pi}{3} \frac{r}{r^2} \sum_{m=-1}^{+1} Y_{1m}(\theta, \phi) Y_{1m}^*(\theta, \phi) \quad (9)$$

For an axial symmetry  $m = 0$ , and the expansion may be further simplified to,

$$r < R \quad \frac{1}{|r-R|} = \frac{r}{R^2} \cos\theta \cos\theta \quad (10)$$

$$r > R \quad \frac{1}{|r-R|} = \frac{R}{r^2} \cos\theta \cos\theta \quad (11)$$

Therefore we have

$$\langle p | \frac{Ze^2}{|r-R|} | s \rangle = N' \frac{4\pi}{3} \frac{\cos\theta}{R} \left[ \int_0^R a b r^4 dr + R^3 \int_R^\infty a b r dr \right] \quad (12)$$

where  $N'$  is a normalization factor,

$$N' = \frac{\sqrt{3}}{4\pi} \frac{1}{\left[ \int_0^\infty a^2(r) r^2 dr \int_0^\infty b^2(r) r^4 dr \right]^{1/2}} \quad (13)$$

The combination of Eq. (12) and (13) then gives Eq. (5).

In Chapter 2 and 5, we have assumed that

$$a(r) = (1 + \alpha r)e^{-\alpha r}$$

$$b(r) = e^{-\beta r}$$

from Eqs. (3), (4) and (5) we find

$$E_s = \frac{3}{14} \alpha^2 + 2 \left[ (-1)^N i \left\{ \frac{2}{R_i} - \frac{1}{7R_i} (2\alpha^3 R_i^3 + 10 \alpha^2 R_i^2 + 19 \alpha R_i + 14) e^{-2\alpha R_i} \right\} \right] \quad (14)$$

$$E_p = \beta^2 + 2 \left[ (-1)^N i \left\{ \frac{2}{R_i} - \frac{1}{3R_i} (2\beta^3 R_i^3 + 6\beta^2 R_i^2 + 9\beta R_i + 6) e^{-2\beta R_i} + \frac{3\cos^2(H)_i - 1}{3\beta^2 R_i^3} \left[ 9 - (2\beta^5 R_i^5 + 6\beta^4 R_i^4 + 12\beta^3 R_i^3 + 18\beta^2 R_i^2 + 18\beta R_i + 9) e^{-2\beta R_i} \right] \right\} \right] \quad (15)$$

$$b = \frac{8}{3\sqrt{7}} \frac{\cos \theta}{R^2} \sqrt{\alpha^3 \beta^5} \left\{ \frac{24}{(\alpha+\beta)^5} + \frac{120\alpha}{(\alpha+\beta)^6} - \frac{3R^3}{(\alpha+\beta)^2} + \frac{12R^2}{(\alpha+\beta)^3} + \frac{24R}{(\alpha+\beta)^4} + \frac{24}{(\alpha+\beta)^5} + \frac{3\alpha R^4}{(\alpha+\beta)^2} + \frac{18\alpha R^3}{(\alpha+\beta)^3} + \frac{60\alpha R^2}{(\alpha+\beta)^4} + \frac{120\alpha R}{(\alpha+\beta)^5} + \frac{120\alpha}{(\alpha+\beta)^6} e^{-(\alpha+\beta)R} \right\} \quad (16)$$

We have also

$$F^+ \text{ centre} : \sum (-1)^{N_i} \frac{2}{R_i} = - \frac{2\alpha_M}{a} \quad (17)$$

$$F_C^+ \text{ centre} : \sum (-1)^{N_i} \frac{2}{R_i} = - \frac{2\alpha_M}{a} + \frac{2}{a} \quad (18)$$

where  $\alpha_M = 1.74756$  is the Madelung constant for the NaCl structure.

The first term in both Eqs. (14) and (15) is the kinetic energy corresponding to the two wavefunctions. Eq. (16) must be interpreted in the following ways: For  $F^+$ -centre,  $b = 0$  because the summation over  $\cos\theta$ , is zero for cubic symmetry; for  $F_C^+$ -centre,  $\cos\theta = 1$  and  $R = a$  if the centre of the charge cloud is assumed to be at the centre of the anion vacancy, otherwise a summation over each shell centred on the anion vacancy is necessary.

In order to calculate the expansions of  $E_{iy}^e$  and  $E_{iz}^e$ , as defined in Chapter 5, to second order in  $\gamma$ , we need the following derivatives. From Eqs. (5.13) and (5.14) we find that

$$\frac{\partial C_s^2}{\partial \gamma} = -2 \frac{b}{\Delta} \frac{\partial b}{\partial \gamma} \frac{1}{\Delta} - \frac{b}{\Delta^2} \frac{\partial \Delta}{\partial \gamma} / \left\{ 1 + 4 \frac{b}{\Delta} \right\}^{3/2} \quad (19)$$

$$\frac{\partial^2 C_s^2}{\partial \gamma^2} = \left\{ \left( -\frac{2}{\Delta^2} + 16 \frac{b^2}{\Delta^4} \right) \left( \frac{\partial b}{\partial \gamma} \right)^2 - \left( \frac{2b}{\Delta^2} + \frac{8b^3}{\Delta^4} \right) \frac{\partial^2 b}{\partial \gamma^2} \right.$$

$$+ \left( \frac{8b}{\Delta^3} + 16 \frac{b^3}{\Delta^5} \right) \frac{\partial b}{\partial \gamma} \frac{\partial \Delta}{\partial \gamma} + \left( \frac{2b^2}{\Delta^3} + 8 \frac{b^4}{\Delta^5} \right) \frac{\partial^2 \Delta}{\partial \gamma^2} + \left( 6 \frac{b^2}{\Delta^4} + 48 \frac{b^4}{\Delta^6} \right) \frac{\partial \Delta}{\partial \gamma} \left. \right\} / \left\{ 1 + 4 \left( \frac{b}{\Delta} \right)^2 \right\}^{5/2}$$

$$\frac{\partial C_p^2}{\partial \gamma} = - \frac{\partial C_s^2}{\partial \gamma} \quad (21)$$

$$\frac{\partial^2 C_p^2}{\partial \gamma^2} = - \frac{\partial^2 C_s^2}{\partial \gamma^2} \quad (22)$$

where  $b$  and  $\Delta$  are defined by Eqs. (5.11) and (5.12). Similarly

$$\frac{\partial C_s C_p}{\partial \gamma} = - \frac{1}{2} \frac{C_s^2 - C_p^2}{C_s C_p} \frac{\partial C_s^2}{\partial \gamma} \quad (23)$$

$$\frac{\partial^2 C_s C_p}{\partial \gamma^2} = - \frac{1}{2} \left\{ 2 \frac{\partial C_s^2}{\partial \gamma} + (C_s^2 - C_p^2) \right. \\ \left. + \frac{\partial C_s C_p}{\partial \gamma} \right\} / C_s C_p \quad (24)$$

After the expansions of  $\frac{\partial V_s}{\partial R_i}$ ,  $\frac{\partial V_p}{\partial R_i}$ ,  $\frac{\partial V_{sp}}{\partial R_i}$  and  $R_i$  in terms of  $\gamma$  are evaluated, we can put

$$C_s^2 \frac{\partial V_s}{\partial R_i} + C_p^2 \frac{\partial V_p}{\partial R_i} - 2C_s C_p \frac{\partial V_{sp}}{\partial R_i} = C_0 + C_1 \gamma + C_2 \gamma^2 \quad (25)$$

and

$$C_p^2 \frac{\partial V_p}{\partial z_i} - 2C_s C_p \frac{\partial V_{sp}}{\partial z_i} = C_0' + C_1' \gamma + C_s' \gamma^2 \quad (26)$$

then the final results for  $E_{ij}^e$  are given by

$$E_{iyo}^e = \frac{y_i}{R_i} C_0 \quad (27)$$

$$E_{iy1}^e = \frac{y_i}{R_i} \left( C_1 - \frac{z_i a}{R_i^2} C_0 \right) \quad (28)$$

$$E_{iy2}^e = \frac{y_i}{R_i} \left\{ C_2 - \frac{z_i a}{R_i^2} C_1 + a^2 \left( \frac{3}{2} \frac{z_i^2}{R_i^4} - \frac{1}{2R_i^2} \right) C_0 \right\} \quad (29)$$

and

$$E_{izo}^e = \frac{z_i C_0}{R_i} + C_0' \quad (30)$$

$$E_{iz1}^e = C_1 \frac{z_i}{R_i} + C_0 \frac{a}{R_i} \left( 1 - \frac{z_i^2}{R_i^2} \right) + C_1' \quad (31)$$

$$E_{iz2}^e = C_0 \frac{a^2}{R_i} \left( \frac{3}{2} \frac{z_i^3}{R_i^4} - \frac{3}{2} \frac{z_i}{R_i^2} \right) + C_1 \frac{a}{R_i} \left( 1 - \frac{z_i^2}{R_i^2} \right) + \frac{z_i}{R_i} C_2 + C_2' \quad (32)$$

In order to calculate the various derivatives of  $C_s^2$  and  $C_p^2$  it is necessary to calculate the expansions of  $E_s$  and  $E_p$  and  $b$  in terms of  $\gamma$ . If we define

$$T = \alpha R, \quad Y = \beta R, \quad D = \alpha + \beta$$

$$ES1(\alpha, R) = \frac{1}{14R^2} (4T^4 + 16T^3 + 28T^2 + 28T + 14)e^{-2T}$$

$$ES2(\alpha, R) = \frac{1}{14R^2} (8T^5 + 24T^4 + 40T^3 + 56T^2 + 56T + 28)e^{-2T}$$

$$EP1(\beta, R) = \frac{1}{6R^2} (4Y^4 + 8Y^3 + 12Y^2 + 12Y + 6)e^{-2Y}$$

$$EP2(\beta, R) = \frac{1}{6R^4} (8Y^5 + 8Y^4 + 16Y^3 + 24Y^2 + 24Y + 12)e^{-2Y}$$

$$FP3(\beta, R) = \frac{1}{6R^6} (16Y^6 + 8Y^5 + 32Y^4 + 64Y^3 + 96Y^2 + 96Y + 48)e^{-2Y}$$

$$EP4(\beta, R) = \frac{1}{R^4} (2Y^5 + 6Y^4 + 12Y^3 + 18Y^2 + 18Y + 9)e^{-2Y}$$

$$EP5(\beta, R) = \frac{1}{R^4} (4Y^6 + 8Y^5 + 18Y^4 + 36Y^3 + 54Y^2 + 54Y + 27)e^{-2Y}$$

$$EP6(\beta, R) = \frac{1}{R^4} (8Y^7 + 8Y^6 + 28Y^5 + 72Y^4 + 144Y^3 + 216Y^2 + 216Y + 108)e^{-2Y}$$

$$ESP\phi(\alpha, \beta, R) = \frac{1}{R^3} \left\{ \left( \frac{3}{D^2} + \frac{18\alpha}{D^3} \right) R^3 + \frac{3\alpha}{D^2} R^4 + \left( \frac{12}{D^3} + \frac{60\alpha}{D^4} \right) R^2 + \left( \frac{24}{D^4} + \frac{120\alpha}{D^5} \right) R + \frac{24}{D^5} + \frac{120\alpha}{D^6} \right\} e^{-DR}$$

$$ESP1(\alpha, \beta, R) = \frac{1}{R^4} \left\{ \frac{3\alpha}{D} R^5 + \frac{3}{D} + \frac{15\alpha}{D^2} R^4 + \frac{12}{D^2} + \frac{60\alpha}{D^3} R^3 + \frac{36}{D^3} + \frac{180\alpha}{D^4} R^2 + \frac{72}{D^4} + \frac{360\alpha}{D^5} R + \frac{42}{D^5} + \frac{360\alpha}{D^6} \right\} e^{-DR}$$

$$ESP2(\alpha, \beta, R) = \frac{1}{R^5} \left\{ 3\alpha DR^6 + \left( 3 + \frac{12\alpha}{D} \right) R^5 + \left( \frac{12}{D} + \frac{60\alpha}{D^2} \right) R^4 + \frac{60}{D^2} + \frac{300\alpha}{D^3} R + \left( \frac{144}{D^3} + \frac{720\alpha}{D^4} \right) R^2 + \left( \frac{288}{D^4} + \frac{1440\alpha}{D^5} \right) R + \left( \frac{288}{D^5} + \frac{144\alpha}{D^6} \right) \right\} e^{-DR}$$

Then the various derivatives can be shown to be given by

$$\frac{\partial E_s}{\partial \gamma} = -\frac{4}{a} + 4a * ES1(\alpha, a) \quad (33)$$

$$\begin{aligned} \frac{\partial^2 E_s}{\partial \gamma^2} &= \frac{8}{a} - 2 \sum (-1)^{N_i} \left\{ \frac{2a^2 z_i^2}{R_i^4} \left(-1 + \frac{z_i^2}{R_i}\right) * ES1(\alpha, R_i) \right. \\ &+ \left. \frac{2a^2 z_i^2}{R_i} * ES2(\alpha, R_i) \right\} \quad (34) \end{aligned}$$

$$\frac{\partial E_p}{\partial \gamma} = 4a \left\{ -\frac{1}{a^2} + EP1(\beta, a) - \frac{9}{\beta^2 a^4} + \frac{1}{3\beta^2} * EP5(\beta, a) \right\} \quad (35)$$

$$\frac{\partial^3 E_p}{\partial \gamma^2} = 4a^2 \left\{ \frac{2}{a^3} + \frac{32 \cdot 877}{2\beta^2 a^5} + \sum (-1)^{N_i} \left[ \frac{78 \cdot 75}{\beta^2} \frac{z_i^4}{R_i^9} + \frac{1}{R_i} \right] \right\}$$

$$\left(1 - \frac{z_i^2}{R_i^2} * EP1(\beta, R_i) - \frac{z_i^2}{R_i} * EP2(\beta, R_i) + \frac{1}{\beta^2 R_i} \left(5 \frac{z_i^2}{R_i^2} - 1 - \frac{4z_i^4}{R_i^4}\right)\right)$$

$$\begin{aligned}
& * EP4(\beta, R_i) + \frac{1}{6\beta^2 R_i} \left( 16 \frac{z_i^2}{R_i^2} - 1 - 15 \frac{z_i^4}{R_i^4} \right) * EPS(\beta, R_i) \\
& - \frac{1}{6\beta^2 R_i} \left( 3 \frac{z_i^4}{R_i^4} - \frac{z_i^2}{R_i^2} \right) * EP6(\beta, R_i) \Bigg\} \quad (36)
\end{aligned}$$

$$\begin{aligned}
\frac{\partial b}{\partial \gamma} = a \left\{ -\frac{32}{3\sqrt{7}} \frac{\sqrt{\alpha^3 \beta^5}}{D^5 a^3} \left( 24 + \frac{120\alpha}{D} \right) + \frac{16}{3\sqrt{7}} \sqrt{\alpha^3 \beta^5} \sum (-1)^{N_i} \right. \\
\left. \left[ \frac{z_i^2}{R_i} * ESP1(\alpha, \beta, R_i) - ESP\phi(\alpha, \beta, R_i) \right] \right\} \quad (37)
\end{aligned}$$

$$\begin{aligned}
\frac{\partial^2 b}{\partial \gamma^2} = \frac{16}{3\sqrt{7}} \sqrt{\alpha^3 \beta^5} \left\{ \frac{6}{a^2 D^5} \left( 24 + \frac{120\alpha}{\alpha + \beta} \right) + 2a^2 * ESP1(\alpha, \beta, a) \right. \\
\left. - a^4 * ESP2(\alpha, \beta, a) \right\} \quad (38)
\end{aligned}$$

where use has been made of the lattice summation by Jones and Ingham<sup>(1)</sup>.

The remaining summations converge rapidly.

#### Reference

1. J.E. Lennard-Jones, and A.E. Ingham, Proc. Roy. Soc.

107 A, 636, (1925).

(B) Electrostatic Field due to the Electron

In chapter 5, we saw that the  $i$ th component of the total electrostatic field at the  $j$ th site is

$$E = E_{ij}^v + E_{ij}^e + E_{ij}^d$$

where  $E_{ij}^v$  are the electrostatic field due to the vacancies,  $E_{ij}^d$  are the electrostatic field due to the ionic displacements and  $E_{ij}^e$  that are due to the electron. Values of this total electrostatic field at the lattice sites shown in Fig. 2, are listed below:-

$$(0,a,0) : E_{2y} = \frac{1.293}{a^2} + E_{2y}^e + \frac{1}{a^2} (-12.726 \sigma + 13.584 \sigma^2)$$

$$E_{2z} = \frac{.707}{a^2} + E_{2z}^e + \frac{1}{a^2} (-3.927 \sigma + 8.375 \sigma^2)$$

$$(0,0,-a) : E_{1z} = \frac{-1.5}{a^2} + E_{1z}^e + \frac{1}{a^2} (15.008 \sigma - 13.065 \sigma^2)$$

$$(0,a,-a) : E_{Ay} = \frac{.53}{a^2} + E_{Ay}^e + \frac{1}{a^2} (-2.534 \sigma - 2.642 \sigma^2)$$

$$E_{Az} = -\frac{.352}{a^2} + E_{Az}^e + \frac{1}{a^2} (2.472 \sigma + 2.464 \sigma^2)$$

$$(a,a,0) : E_{By} = \frac{.324}{a^2} + E_{By}^e + \frac{1}{a^2} (-1.732 \sigma - 2.252 \sigma^2)$$

$$E_{Bz} = \frac{.384}{a^2} + E_{Bz}^e + \frac{1}{a^2} (-.408 \sigma - 1.136 \sigma^2)$$

$$(0, a, a) : E_{3y} = \frac{-1.293}{a^2} + E_{3y}^e + \frac{1}{a^2} (5.99 \sigma - 13.272 \sigma^2)$$

$$E_{3z} = \frac{.707}{a^2} + E_{3z}^e + \frac{1}{a^2} (-4.233 \sigma + 6.851 \sigma^2)$$

$$(0, 0, 2a) : E_{4z} = \frac{-1.5}{a^2} + E_{4z}^e + \frac{1}{a^2} (7.98 \sigma - 12.359 \sigma^2)$$

(C) Wave Function of the  $F_C^+$ -electron in the Continuum Model

If we define

$$M(\mu) = e^{-P\mu} \sum_{\ell=0}^4 f_{\ell} P_{\ell}(\mu)$$

$$L(\lambda) = e^{-\frac{x}{2}} \sum_{n=0}^4 \frac{C_n}{n!} L_n(x)$$

then the total wave function of the ground state is

$$\phi = N M(\mu) L(\lambda)$$

where  $N$  is a normalisation constant, and the parameters  $p$  and  $\lambda$  are given in Chapter 4.

The normalization constant and the coefficients of expansion  $f_l$  and  $C_n$  are given in the following table:

	N	$\frac{f_1}{f_0}$	$\frac{C_1}{C_0}$	$\frac{f_2}{f_0}$	$\frac{C_2}{C_0}$	$\frac{f_3}{f_0}$	$\frac{C_3}{C_0}$	$\frac{f_4}{f_0}$	$\frac{C_4}{C_0}$
MgO	.121	-1.029	.161	.193	.042	.006	.014	-.0001	.005
CaO	.101	-1.031	.157	.191	.040	-.005	.013	-.0001	.005
SrO	.094	-1.033	.148	.186	.036	-.004	.011	-.0001	.004
BaO	.081	-1.030	.159	.192	.041	-.006	.013	-.0001	.005

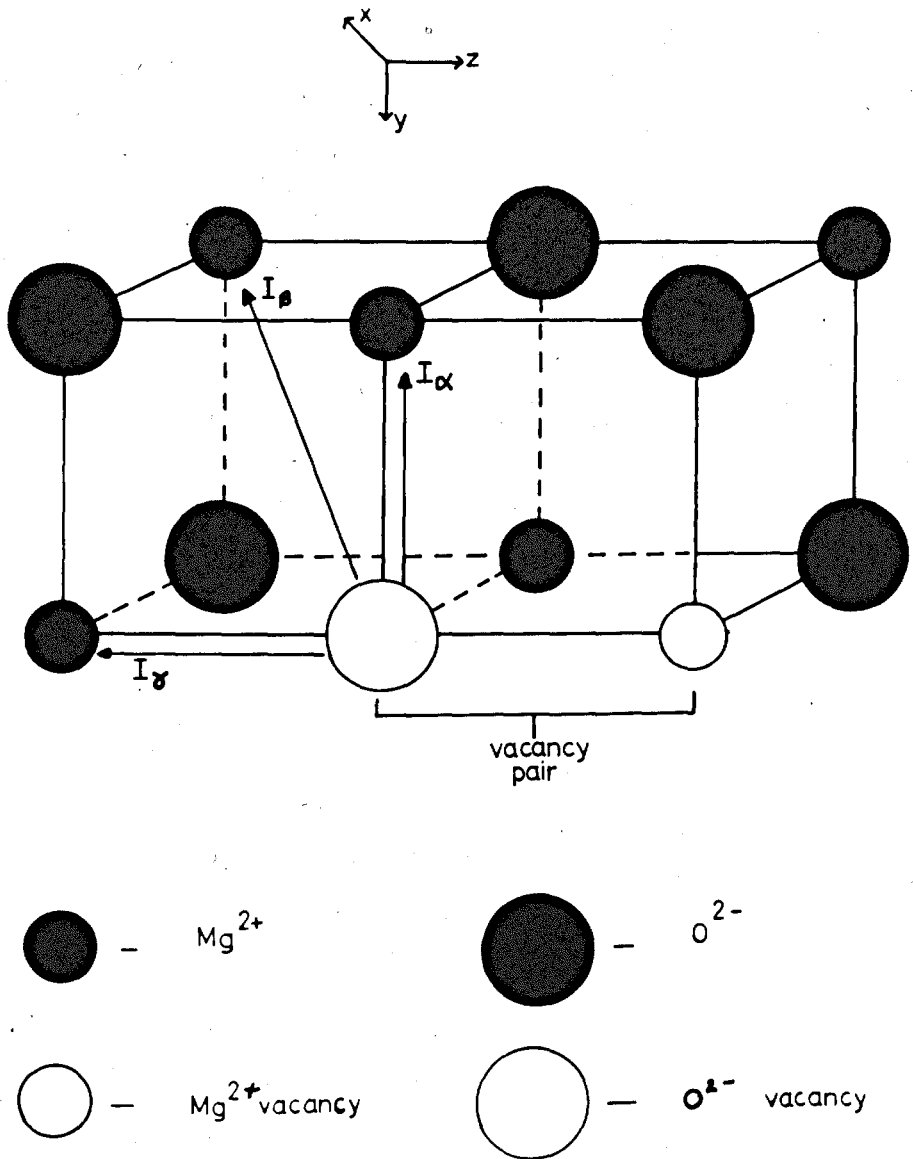


Figure 1A

The divacancy nature and the most important hyperfine interactions of the  $F_C^+$  centre are shown

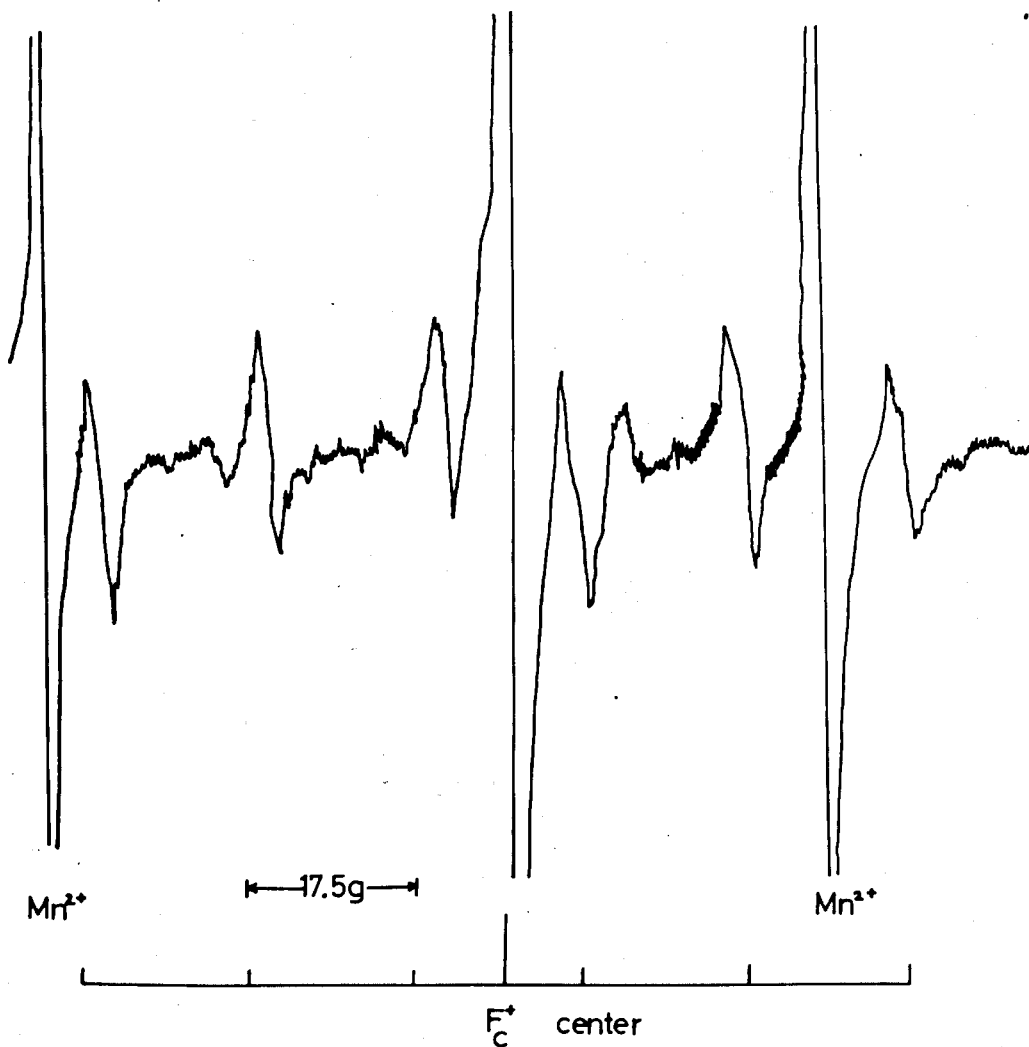


Figure 1B

The hyperfine structure in the electron-spin-resonance spectrum of the  $F_C^+$  center is shown. The measurement was made at  $77^\circ K$  with  $H_0 \parallel [111]$  crystal axis and at a microscope frequency of  $9.2 Gc/sec$ .

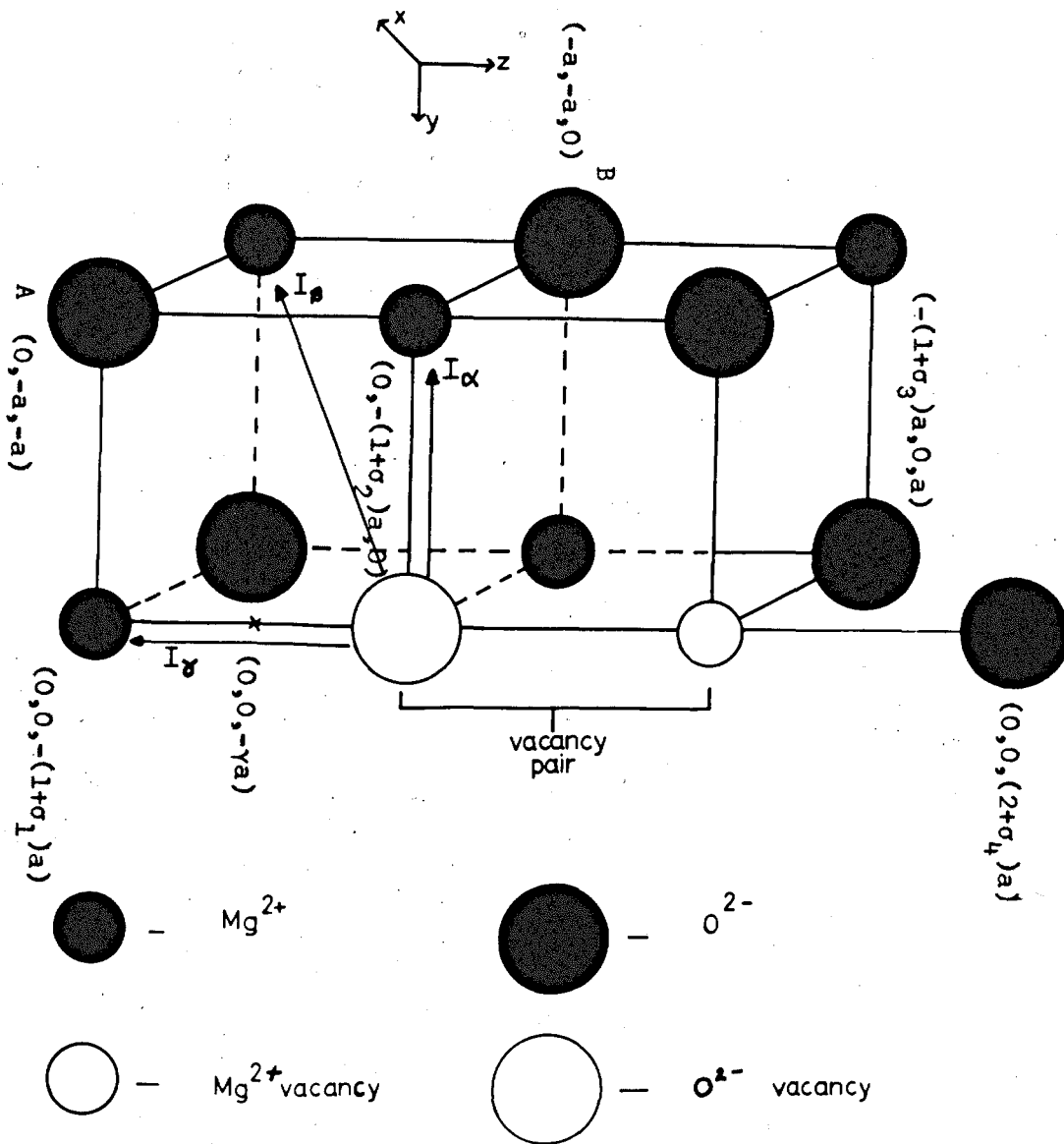


Figure 2

Relevant ionic arrangements neighbouring the divacancy at  $(0,0,0)$  and  $(0,0,a)$ . The divacancy axis is along the  $z$  axis with the anion vacancy at the origin of the coordinate system. In the figure the anions at A and B are not allowed to move, while for all other ions  $\sigma_1 = \sigma_2 = \sigma_3 = \sigma_4 = \sigma$ . The trapped electron is assumed to be at  $(0,0,-\gamma a)$ .

Table 1A

Kemp and Neeley's LCAO results on  $F^+$ -centres in MgO

In the absence of polarization and lattice distortion correction:

$$\Gamma_1 : E_S = -19.1 \text{ eV}$$

$$\Delta E = 4.7 \text{ eV}$$

$$\Gamma_4' : E_P = -14.4 \text{ eV}$$

In the presence of Lattice distortion alone

$$\sigma_0 = +0.072 \quad \Delta W_S = 4.85 \text{ eV}$$

$$\Delta E = 4.34 \text{ eV}$$

$$\Delta W_P = 4.49 \text{ eV}$$

In the presence of Polarization alone

$$\sigma_0 = 0 \quad E_S = -15.2 \text{ eV}$$

$$\Delta E = 4.7 \text{ eV}$$

$$E_P = -10.5 \text{ eV}$$

In the presence of both polarization and lattice distortion

$$\sigma_0 = +0.05 \quad E_S = -12.9 \text{ eV}$$

$$\Delta E = 4.7 \text{ eV}$$

$$E_P = -8.2 \text{ eV}$$

$$\text{Experimental value } \Delta E = 4.95 \text{ eV}$$

Table 1B

Neeley's results on the  $F^+$ -centre in the Alkaline Earth Oxides (obtained using Gaussian wave functions).

	$\sigma_o$	$\Delta E_S^*$	$E_S$	$E_P$	$\Delta E$	Expt <sup>†</sup>
MgO	.04	6.39	-12.64	-8.11	4.53	4.95
CaO	.02	6.42	-10.63	-7.08	3.55	3.7
SrO	.01	6.47	-9.66	-6.49	3.17	3.0
BaO	-.01	6.52	-8.65	-5.84	2.81	2.0

\*  $\Delta E_S$  is the polarisation and lattice distortion correction to the ground state energy  $E_S$ .  $\sigma_o$  is the lattice distortion.

† Experimental values are taken from B. Henderson and J.E. Wertz, *Advances in Physics*, 17, No. 70, 749, (1968).

TABLE 2

Comparison of calculated F-band energies (Ry) in  
alkali halides with experimental values measured at 77°K.<sup>a,b</sup>  
The compounds are listed in ascending order of the ratio of  
ionic radii,  $R(=r_-/r_+)$ .

Compound	$\Delta E_{\text{theory}}$	$\Delta E_{\text{exp}}^{(a)}$	$\Delta E_{\text{exp}}^{(b)}$
CsF	0.135	0.139	0.139
RbF	0.169	0.178	0.179
KF	0.202	0.210	0.206
RbCl	0.140	0.150	0.149
RbBr	0.128	0.136	0.136
NaF	0.278	0.276	0.274
KCl	0.161	0.169	0.172
KBr	0.146	0.154	0.153
RbI	0.121	0.125	0.126
KI	0.135	0.136	0.138
NaCl	0.201	0.202	0.204
LiF	0.386	0.377	0.378
NaBr	0.176	0.174	0.173
NaI	0.160	0.153	...
LiCl	0.242	0.241	0.243
LiBr <sup>c</sup>	0.208	...	0.199
LiI	0.184	...	0.240

a. C.J. Buchenauer and D.B. Fitchen

b. A.E. Hughes, D. Pooley, H.V. Rahman and W.A. Runciman

Table 3

$F^+$ -centre energies after polarisation and lattice distortion correction for the alkaline earth oxides (using wave functions given in §2).

	$\sigma_o$	$E_S$	$E_S(\sigma_o)$	$E_P$	$E_P(\sigma_o)$	$\Delta E$	$\Delta E(\sigma_o)$	Expt*
MgO	.048	-18.207	-13.185	-12.56	-8.389	5.647	4.796	4.95
CaO	.059	-16.371	-10.77	-11.765	-6.038	4.606	3.731	3.7
SrO	.064	-15.487	-9.76	-11.343	-6.473	4.144	3.287	3.0
BaO	.063	-14.601	-8.654	-10.896	-5.789	3.705	2.865	2.0

Notation:  $E_S(\sigma_o)$ ,  $E_P(\sigma_o)$  and  $\Delta E(\sigma_o)$  are the binding, excited state and transition energy (in eV) respectively in the presence of polarisation and lattice distortion correction.

Table 4A

Variational and lattice parameters of the Alkaline Earth Oxides

	Variational Parameters		Variational parameter after ion size correction		Polarisabilities		ion size parameters		Lattice parameter a c
	$\alpha$	$\beta$	$\alpha$	$\beta$	$\alpha^+$	$\alpha^-$	A Y	B Y	
MgO	.811	.705	.888	.814	.648	11.126	37.66	12.64	3.975
CaO	.730	.643	.825	.761	3.229	15.956	76.57	43.43	4.54
SrO	.692	.613	.784	.727	5.809	17.347	96.18	65.39	4.86
BaO	.654	.582	.755	.708	10.47	20.603	137.12	110.34	5.22

Note: All parameters are in Rydbergs atomic units.

Table 4B

F<sup>+</sup>-centres energies after ion size corrections for the Alkaline Earth Oxides

	$\sigma_o$	$E_s$	$E_s(\sigma_o)$	$E_p$	$E_p(\sigma_o)$	$\Delta E$	$\Delta E(\sigma_o)$	Expt. $\Delta E$
MgO	.049	-16.957	-11.133	-9.784	-4.25	7.173	6.883	4.95
CaO	.059	-15.087	-8.127	-8.886	-.429	6.201	7.698	3.7
SrO	.064	-14.340	-8.179	-8.729	-.231	5.611	7.948	3.0
BaO	.068	-13.461	-9.289	-8.221	-1.147	5.24	8.142	2.0

Note all energies in ev.

Table 5

Pincherle's results on D-centre

	a(A.U.)	Z	$K_V$	$\beta$	$\mu$	$\lambda$	E(ev)
AgBr	5.44	1	4.62	2.35	$0.73+0.43\lambda^2$	.051	-.005
PbS	5.64	2	6	3.75	$1.54+0.50\lambda^2$	.40	-.27

Table 5A

Wertz's experimental results of g values for F-centres and  $F_2$ -centres in powders.

Powder	g(F-centre)	g( $F_2$ -centre)
MgO	2.0023	2.0008
CaO	2.0001	1.9995
SrO	1.9846	1.981 <sub>6</sub>
BaO	1.936*	

\* Values taken from Carson et al.

Table 6

Energies of the  $F_C^+$ -centres in the Alkaline Earth Oxides  
in the continuum model.

	MgO	CaO	SrO	BaO
$\epsilon_\infty$	2.95	3.28	3.31	3.83
$E_b$	2.02	1.72	1.70	1.24
$E_b/E_{\text{gap}}$	.232	.224	.254	.248
Expt. $E_b$	3.60			

Table 7

Hyperfine constants of the  $F_C^+$ -centre in the continuum model.

	(0,0,-1)			(0,1,0)			(1,1,-1)		
	H.F.	S.O.	Expt	H.F.	S.O.	Expt	H.F.	S.O.	Expt
MgO	18.07	5.54	17.5	9.110	2.79	-2.	.798	.245	<1.
CaO	40.24	4.22		20.34	2.13		1.58	.166	
SrO		1.99			1.01			.06	
BaO		5.41			2.73			.23	

H.F = Hartree Fock wave functions, S.O = Slater Orbitals. All results are in units of Gauss

Table 8

Binding Energies of the  $F_C^+$ -centre in the Alkaline Earth Oxides before polarisation, distortion and ion size corrections.

	Variational Parameters		$E_b^*$	Expt. $E_b$
	$\alpha$	$\beta$	ev.	ev
MgO	.723	.695	-7.286	-3.6
CaO	.651	.631	-6.799	
SrO	.616	.600	-6.542	
BaO	.582	.568	-6.271	

\* The  $E_b$  as given are referred to the vacuum level. In order to compare with the experimental result, a knowledge of the energy of the bottom of the conduction band is needed. For MgO the bottom of the conduction band is about  $\sim -1$  ev.

Table 9

The binding energies of the  $F_C^+$ -centre with polarisation and lattice distortion correction.

	$\sigma_0$	$\gamma$	$E_0$ ev	Lattice distortion $\Delta E_L$ ev	Polarisation $\Delta E_p$ ev	$E_b^*$ ev	Expt ev
MgO	.028	.110	-7.286	1.013	-0.621	-6.893	-3.5
CaO	.027	.124	-6.799	.832	-0.398	-6.365	
SrO	.026	.131	-6.542	.731	-0.245	-6.056	
BaO	.024	.140	-6.271	.632	-0.102	-5.741	

\* See footnote of Table 8

Table 10

Dipole moments and Electrostatic fields due to the  $F_C^+$ -electron

	$E_{2y}$	$P_{2y}$	$E_{2z}$	$P_{2z}$	$E_{1z}$	$P_{1z}$	$E_{4z}$	$P_{4z}$	$E_{By}$	$P_{By}$	$E_{Bz}$	$P_{Bz}$	$E_{Ay}$
MgO	-.043	.022	-.02	.009	.073	-0.0	-0.01	-0.728	-0.019	.029	-.009	.142	-.035
CaO	-.033	0.083	-.016	.036	.06	0.01	-.008	-.813	-.015	.023	-.007	.147	-.028
SrO	-.029	.129	-.014	.059	.053	.026	-.007	-.801	-.013	.013	-.006	.134	-.025
BaO	-.025	.203	-.012	.094	0.048	.058	-.006	-.837	-.011	.005	-0.005	.129	-.022

	$P_{Ay}$	$E_{Az}$	$P_{Az}$	$E_{3y}$	$P_{3y}$	$E_{3z}$	$P_{3z}$
MgO	-.053	.022	0.041	-.011	-0.694	-0.017	0.187
CaO	-.078	.017	.053	-.008	-.782	-.013	.218
SrO	-.087	0.015	.055	-.007	-.771	-.011	.219
BaO	-.106	0.013	.062	-.006	-.813	-.01	.236

Notations: For the electrostatic field  $E_{ij}$ ,  $i$  stands for the lattice site and  $j$  the cartesian component as indicated e.g.  $y$  or  $z$ . Similarly for the dipole moments. See Figures in Chapter 5 for the lattice sites concerned.

Table 11

Binding Energies of the  $F_C^+$ -centres after ion size corrections.

	$E_b$ ev	$\Delta E_b$ ev	$E_f$ ev	Conduction band minima ev	E ev	Expt. E ev
MgO	-6.893	1.741	-5.153	~-1.	~-4.1	-3.6
CaO	-6.365	1.822	-4.543			
SrO	-6.056	1.654	-4.402			
BaO	-5.741	1.677	-4.064			

---

Note:  $E_b$  are the energies after polarisation and lattice distortion correction are included as shown in Table 9.  $\Delta E_b$  are the ion size corrections while  $E_f$  are the binding energies referred to the vacuum and E the binding energies referred to the bottom of the conduction band.

Table 12

Hyperfine constants of the  $F_C^+$ -centre in the Alkaline Earth Oxides

	(0,0,-1)				(0,1,0)				(1,1,-1)				ratio $A_{00-1}/A_{010}$				
	P.I.	L+P <sub>o</sub>	L+P <sub>o</sub> +I	Expt.	P.I.	L+P <sub>o</sub>	L+P <sub>o</sub> +I	Expt.	P.I.	L+P <sub>o</sub>	L+P <sub>o</sub> +I	Expt.	P.I.	L+P <sub>o</sub>	L+P <sub>o</sub> +I	Expt.	
MgO	H.F.	42.62	54.29	42.75	17.5	11.05	8.05	6.98	-2.0	1.10	1.28	.60	<1.	3.86	6.75	6.14	-8.
	S.O.	13.00	16.57	13.08		3.37	2.45	2.14		.34	.39	.18		3.86	6.75	6.14	
CaO	H.F.	103.45	143.37	101.84		25.69	18.18	13.64		2.34	2.84	1.00		4.03	7.9	7.46	
	S.O.	10.99	15.25	10.73		2.76	1.93	1.44		.25	.30	.11		4.03	7.9	7.46	
SrO	H.F.																
	S.O.	6.33	9.34	6.29		1.56	1.09	.76		.13	.17	.05		4.06	8.56	8.28	
BaO	H.F.																
	S.O.	15.63	26.12	13.99		3.79	2.75	1.48		.31	.43	.09		4.13	9.5	9.46	

P.I. represent the results from a point ion calculation;  
 L+P = P.I. with lattice distortion and polarisation correction;  
 L+P<sup>o</sup>+I = L+P<sup>o</sup> with ion size correction as explained in the text  
 H.F.<sup>o</sup> and S.O.<sup>o</sup> have the same meaning as in Table 7.